

AD\_\_\_\_\_

Award Number: W81XWH-12-1-0533

TITLE: Role of TAF12 in the Increased VDR Activity in Paget's Disease of Bone

PRINCIPAL INVESTIGATOR: Kurihara, Noriyoshi

CONTRACTING ORGANIZATION: Indiana University School of Medicine  
Indianapolis, IN 46202-5167

REPORT DATE: October 2013

TYPE OF REPORT: Annual Report

PREPARED FOR: U.S. Army Medical Research and Materiel Command  
Fort Detrick, Maryland 21702-5012

DISTRIBUTION STATEMENT: Approved for Public Release;  
Distribution Unlimited

The views, opinions and/or findings contained in this report are those of the author(s) and should not be construed as an official Department of the Army position, policy or decision unless so designated by other documentation.

<b>REPORT DOCUMENTATION PAGE</b>				<i>Form Approved</i> <b>OMB No. 0704-0188</b>	
<small>Public reporting burden for this collection of information is estimated to average 1 hour per response, including the time for reviewing instructions, searching existing data sources, gathering and maintaining the data needed, and completing and reviewing this collection of information. Send comments regarding this burden estimate or any other aspect of this collection of information, including suggestions for reducing this burden to Department of Defense, Washington Headquarters Services, Directorate for Information Operations and Reports (0704-0188), 1215 Jefferson Davis Highway, Suite 1204, Arlington, VA 22202-4302. Respondents should be aware that notwithstanding any other provision of law, no person shall be subject to any penalty for failing to comply with a collection of information if it does not display a currently valid OMB control number. <b>PLEASE DO NOT RETURN YOUR FORM TO THE ABOVE ADDRESS.</b></small>					
<b>1. REPORT DATE</b> October 2013		<b>2. REPORT TYPE</b> Annual		<b>3. DATES COVERED</b> 30 September 2012 - 29 September 2013	
<b>4. TITLE AND SUBTITLE</b> Role of TAF12 in the Increased VDR Activity in Paget's Disease of Bone				<b>5a. CONTRACT NUMBER</b>	
				<b>5b. GRANT NUMBER</b> W81XWH-12-1-0533	
				<b>5c. PROGRAM ELEMENT NUMBER</b>	
<b>6. AUTHOR(S)</b> Kurihara, Noriyoshi  email:norikuri@iupui.edu				<b>5d. PROJECT NUMBER</b>	
				<b>5e. TASK NUMBER</b>	
				<b>5f. WORK UNIT NUMBER</b>	
<b>7. PERFORMING ORGANIZATION NAME(S) AND ADDRESS(ES)</b> Indiana University School of Medicine Indianapolis, IN 46202-5167				<b>8. PERFORMING ORGANIZATION REPORT NUMBER</b>	
<b>9. SPONSORING / MONITORING AGENCY NAME(S) AND ADDRESS(ES)</b> U.S. Army Medical Research and Materiel Command Fort Detrick, Maryland 21702-5012				<b>10. SPONSOR/MONITOR'S ACRONYM(S)</b>	
				<b>11. SPONSOR/MONITOR'S REPORT NUMBER(S)</b>	
<b>12. DISTRIBUTION / AVAILABILITY STATEMENT</b> Approved for Public Release; Distribution Unlimited					
<b>13. SUPPLEMENTARY NOTES</b>					
<b>14. ABSTRACT</b>  See below					
<b>15. SUBJECT TERMS-</b> none provided					
<b>16. SECURITY CLASSIFICATION OF:</b>			<b>17. LIMITATION OF ABSTRACT</b>  UU	<b>18. NUMBER OF PAGES</b>  52	<b>19a. NAME OF RESPONSIBLE PERSON</b> USAMRMC
<b>a. REPORT</b> U	<b>b. ABSTRACT</b> U	<b>c. THIS PAGE</b> U			<b>19b. TELEPHONE NUMBER</b> (include area code)

**[SF298]**

**Note: An abstract is required to be provided in Block 14**

Osteoclast (OCL) precursors from 70% of Paget's disease (PD) patients express measles virus nucleocapsid protein (MVNP) and are hypersensitive to 1,25-dihydroxyvitamin D<sub>3</sub> (1,25-(OH)<sub>2</sub>D<sub>3</sub>; also known as calcitriol). The increased 1,25-(OH)<sub>2</sub>D<sub>3</sub> sensitivity is mediated by transcription initiation factor TFIID subunit 12 (TAF12), a coactivator of the vitamin D receptor (VDR), which is present at much higher levels in *MVNP*-expressing OCL precursors than normals. These results suggest that TAF12 plays an important role in the abnormal OCL activity in PD. However, the molecular mechanisms underlying both 1,25-(OH)<sub>2</sub>D<sub>3</sub>'s effects on OCL formation and the contribution of TAF12 to these effects in both normals and PD patients are unclear. Inhibition of TAF12 with a specific TAF12 antisense construct decreased OCL formation and OCL precursors' sensitivity to 1,25-(OH)<sub>2</sub>D<sub>3</sub> in PD patient bone marrow samples. Further, OCL precursors from transgenic mice in which TAF12 expression was targeted to the OCL lineage (tartrate-resistant acid phosphatase [TRAP]-TAF12 mice), formed OCLs at very low levels of 1,25-(OH)<sub>2</sub>D<sub>3</sub>, although the OCLs failed to exhibit other hallmarks of PD OCLs, including receptor activator of NF-κB ligand (RANKL) hypersensitivity and hypermultinucleation. Chromatin immunoprecipitation (ChIP) analysis of OCL precursors using an anti-TAF12 antibody demonstrated that TAF12 binds the 24-hydroxylase (*CYP24A1*) promoter, which contains two functional vitamin D response elements (VDREs), in the presence of 1,25-(OH)<sub>2</sub>D<sub>3</sub>. Because TAF12 directly interacts with the cyclic adenosine monophosphate-dependent activating transcription factor 7 (ATF7) and potentiates ATF7-induced transcriptional activation of ATF7-driven genes in other cell types, we determined whether TAF12 is a functional partner of ATF7 in OCL precursors. Immunoprecipitation of lysates from either wild-type (WT) or *MVNP*-expressing OCL with an anti-TAF12 antibody, followed by blotting with an anti-ATF7 antibody, or vice versa, showed that TAF12 and ATF7 physically interact in OCLs. Knockdown of ATF7 in *MVNP*-expressing cells decreased cytochrome P450, family 24, subfamily A, polypeptide 1 (*CYP24A1*) induction by 1,25-(OH)<sub>2</sub>D<sub>3</sub>, as well as TAF12 binding to the *CYP24A1* promoter. These results show that ATF7 interacts with TAF12 and contributes to the hypersensitivity of OCL precursors to 1,25-(OH)<sub>2</sub>D<sub>3</sub> in PD.

## Table of Contents

	<u>Page</u>
1. Introduction	1
2. Keywords	1
3. Overall Project Summary	1
4. Key Research Accomplishments	5
5. Conclusion	5
6. Publications, Abstracts, and Presentations	5
7. Inventions, Patents and Licenses	6
8. Reportable Outcomes	6
9. Other Achievements	6
10. References	6
11. Appendices	6

## **1. INTRODUCTION:**

Vitamin D is a key regulator of bone homeostasis, but its effects on osteoclasts (OCLs) beyond the capacity of 1,25-(OH)<sub>2</sub>D<sub>3</sub> to induce RANKL and decrease OPG in stromal cells are unclear. We previously reported that OCL precursors from PD patients are hypersensitive to 1,25-(OH)<sub>2</sub>D<sub>3</sub> and form OCLs at physiologic rather than pharmacologic levels of vitamin D. We found that the increased 1,25-(OH)<sub>2</sub>D<sub>3</sub> sensitivity is mediated by TAF12, a novel coactivator of VDR, and plays an important role in the abnormal OCL activity in Paget's Disease (PD). Further, increased expression of TAF12 in NIH3T3 cells or marrow stromal cells also increases their sensitivity to 1,25-(OH)<sub>2</sub>D<sub>3</sub>, indicating that TAF12 can act as a VDR coactivator in multiple cell types. However, the molecular mechanisms underlying both vitamin D<sub>3</sub>'s effects on OCL formation and the contribution of TAF12 to these effects in both normals and PD patients are undefined. Since PD represents one of the most exaggerated examples of coupled bone remodeling, studies of PD provide a paradigm for understanding the molecular mechanisms regulating both normal and pagetic OCL and osteoblast activity. Therefore, we will examine the mechanisms of action of TAF12 on VDR-mediated transcription in OCL precursors (OCL-P), CD11b purified marrow cells and the effects of deletion of TAF12 on bone remodeling and the development of PD in Measles Virus Nucleocapsid Protein (MVNP) expressing OCL-P as a PD model system, which develops PD-like OCLs and bone lesions.

## **2. KEYWORDS:**

TAF12, Paget's bone disease, Measles virus nucleocapsid protein (MVNP), ATF7, TAF4, Osteoclast (OCL), VDR, CYP24A1

## **3. OVERALL PROJECT SUMMARY:**

**Aim1. Determine the mechanism(S) whereby TAF12 enhances cellular responsiveness to 1,25-(OH)<sub>2</sub>D<sub>3</sub>/VDR-mediated transcription in osteoclast(OCL) precursors.**

**Task 1A. Determine if increased VDR content enhances 1,25-(OH)<sub>2</sub>D<sub>3</sub> sensitivity of OCL precursors and if TAF4 and ATF7 contribute to TAF12's capacity to increase VDR content.**

**1A1. Determine if increased VDR content contributes to the 1,25-(OH)<sub>2</sub>D<sub>3</sub> hypersensitivity of OCL precursors, and if ATF7, which binds TAF12, is required for TAF12 or 1,25-(OH)<sub>2</sub>D<sub>3</sub> to increase VDR half-life.**

In this Aim, we determined the roles that TAF12 and ATF7 play in VDR mediated transcription in OCL-P. Further, how ATF7 interacts with TAF12 to regulate VDR mediated transcription has not been previously studied. We clarified the interaction of ATF7 and TAF12 in OCL formation and 1,25-(OH)<sub>2</sub>D<sub>3</sub> hypersensitivity.

**Interaction of TAF12 and ATF7 but not TAF4 affects VDR responsivity:** We determined if ATF7 contributed to the effects of TAF12 on VDR responsivity. Increased levels of ATF7 expression were detected in MVNP expressing OCL-P compared to WT lysates and were not further increased by 1,25-(OH)<sub>2</sub>D<sub>3</sub> (Figure 1A). Expression of TAF4 was not affected by MVNP (Figure 1A). In subsequent experiments, we focused on the interaction of ATF7 and TAF12.

Immunoprecipitation of lysates from OCL precursors of either WT or TRAP-MVNP derived OCL-P with an anti-TAF12 antibody followed by blotting with an anti-ATF7 antibody or vice versa revealed that TAF12 and ATF7 physically interacted in OCL precursors (Figure 1B). Thus, TAF12 is a functional partner of ATF7. We detected increased levels of ATF7 expression in MVNP expressing OCL-P compared to WT OCL precursor lysates that were not further increased by 1,25-(OH)<sub>2</sub>D<sub>3</sub>. Expression of TAF4 was not affected by MVNP. Co-immunoprecipitation studies revealed that TAF12 and ATF7 physically interact in both TRAP-MVNP and WT OCL precursors (Figure 1B), and, thus enhance ATF7-TAF12 interactions.

**ATF7 contribution to TAF12's capacity to increase VDR content:** VDR content in OCL precursors from ATF7 shRNA or control shRNA transduced TRAP-MVNP derived OCL-P were measured after treatment with 1,25-(OH)<sub>2</sub>D<sub>3</sub> (10<sup>-8</sup>M) at 24 and 48 hours. VDR content was markedly decreased in ATF7 shRNA-transduced OCL-P as compared to control shRNA transduced cells (Figure 1C). Since VDR content of ATF7 shRNA transduced OCL-P was very low as shown Figure 1C, examination of the half life of VDR in these cells was technically difficult and could not contribute to TAF12's capacity to increase VDR content and thus could not provide data for original Aim 1A task 1A.

**The Effects of ATF7 on OCL Formation:** We examined the role of ATF7 in osteoclast formation stimulated by 1,25-(OH)<sub>2</sub>D<sub>3</sub>. Treatment of OCL precursors from MVNP or WT mice with an ATF7 shRNA significantly decreased the numbers of TRAP(+) MNC (Figure 1D). Vehicle treated cultures did not form OCL (data not shown). Further, knockdown of ATF7 in OCL precursors from TRAP-MVNP mice decreased CYP24A1 sensitivity to 1,25-(OH)<sub>2</sub>D<sub>3</sub> and TAF12 levels in MVNP-expressing cells.

**Task 1B. Determine the role of TAF12-ATF7/TAF4 interactions in 1,25-(OH)<sub>2</sub>D<sub>3</sub> hypersensitivity.**

**1B1. Determine if functional interactions between ATF7, TAF12 and VDR are involved in the 1,25-(OH)<sub>2</sub>D<sub>3</sub> of OCL precursors, and if TAF4, which enhances recruitment of TFIID by VDR and binds both TAF12 and ATF7, modulates the 1,25-(OH)<sub>2</sub>D<sub>3</sub> hypersensitivity of TAF12-expressing OCL precursors.**

**1B2. Determine if the effects of TAF12 on VDR-mediated transcription of *CYP24A1* is ATF7 and/or TAF4-dependent.**

ChIP analysis was performed using an anti-TAF12 antibody and primers flanking the two VDREs in the *CYP24A1* promoter in both TRAP-MVNP and WT OCL precursors. 1,25-(OH)<sub>2</sub>D<sub>3</sub> was found to induce TAF12 binding to the *CYP24A1* promoter in TRAP-MVNP as well as WT OCL precursors. Both basal and induced levels of VDRE binding were much higher in the TRAP-MVNP OCL precursors (Figure 2A).

To further to clarify the role of ATF7 in the increased VDR responsiveness induced by TAF12 and the effects TAF12 binding to VDR/VDRE, ATF7 was knocked-down in OCL precursors from TRAP-MVNP and WT mice with *ATF7* shRNA. ChIP analysis of ATF7 knock-down in OCL precursors from TRAP-MVNP mice showed markedly decreased TAF12 binding at the *CYP24A1* promoter than control shRNA transduced osteoclast precursors (Figure 2B). Figure 1A shows TAF4 levels in TRAP-MVNP and WT OCL-P. Because there was no effect on TAF4 level, we have not examined TAF4 knockdown in OCL-P from TRAP-MVNP and WT (this differs from our original Aim 1B2).

We showed that knockdown of *ATF7* decreases *CYP24A1* sensitivity to 1,25-(OH)<sub>2</sub>D<sub>3</sub> as well as *TAF12* levels in MVNP-expressing cells (Figure 2B), and knockdown of *ATF7* in OCL precursors decreased OCL formation stimulated by 1,25-(OH)<sub>2</sub>D<sub>3</sub> (Figure 1D). Thus, the interaction of ATF7 with TAF12 may be involved in the up-regulation of TAF12 and the resulting hyper-sensitivity of OCL precursors to 1,25-(OH)<sub>2</sub>D<sub>3</sub>. Our results from ChIP assays of *ATF7* shRNA-treated osteoclast precursors derived from TRAP-MVNP mice show that ATF7 increases TAF12 binding to VDREs and enhances transcriptional activity on *CYP24A1*.

## **Methods**

**ATF7 shRNA transduction** :Non-adherent bone marrow cells from TRAP-MVNP and WT mice were transduced with ATF7 shRNA (NM\_146065) (Sigma-Aldrich) or control shRNA (Sigma-Aldrich) which were designed by MISSION®. The shRNA Lentiviral transduction particles (Sigma-Aldrich) were used for transduction. The transduction was performed by the MagnetoFection™-ViroMag R/L methods (OZ Biosciences), according to the manufacturer's instructions (1, 2). To increase the transduction

efficiency, the cells were plated the day before transduction in 96 well culture plate in the presence of 10 ng/ml of M-CSF and 2  $\mu$ l of ViroMag R/L beads in 50  $\mu$ l of  $\alpha$ MEM 10%FCS containing 10 ng/ml of M-CSF, 500 MOI of Lentiviral transduction particles were added, and the cells incubated for 15 min at room temperature. Then 50  $\mu$ l of virus particles/magnet were mixed in each well and cells were incubated on a magnet plate for 60 min. The culture plates were removed from the magnetic plate and cells were cultured with or with 1,25-(OH)<sub>2</sub>D<sub>3</sub> (10<sup>-8</sup> M) for 7 days. The level of OCL formation was determined by counting the number of TRAP(+) multinucleated cells ( $\geq 3$  nuclei/cell).

**ChIP assays:** ChIP assays were performed as described previously using osteoclast precursors from TRAP-MVNP or WT mice (3, 4). The equivalent of 10  $\mu$ g DNA was used as starting material (input) in each ChIP reaction. The DNA was fragmented by sonification and then immuno-precipitated with 2  $\mu$ g of anti-TAF12 antibody (Protein Tech Group, Inc). Portions of the ChIP DNA fractions (5%) or starting DNA (0.02%–0.05%) were used for PCR analysis. The reaction was performed with AmpliTaq Gold DNA Polymerase (Applied Biosystems) for 35 cycles of 60 seconds at 95°C, 90 seconds at 58°C, and 120 seconds at 68°C. The gene-specific primers for mouse CYP24A1 mRNA were 5'-ATT ACC TGA GAA TCA GAG GCC ACG-3' (sense) and 5'-GCC AAA TGC AGT TTA AGC TCT GCT-3' (antisense). The PCR products were separated on 2% agarose gels and visualized with ultraviolet light. All ChIP assays were repeated at least 3 times.

### Figure Legends:

**Figure 1. Functional interaction between ATF7 and TAF12:** **(A)** Expression of TAF12, ATF7 and TAF4 in OCL precursors from WT and TRAP-MVNP mice. CD11b<sup>+</sup> marrow mononuclear cells from WT and TRAP-MVNP mice were cultured with  $\alpha$ MEM-10% FCS for 3 days, and then 10<sup>-10</sup> M 1,25-(OH)<sub>2</sub>D<sub>3</sub> or vehicle was added for 48 hours. The cell lysates were collected and the nuclear fraction was isolated using a nuclear isolation kit (Active Motif) and analyzed by Western blot for effects of MVNP on TAF12, ATF7 and TAF4 levels. **(B)** TAF12 binds ATF7 in OCL precursors. Cell extracts from WT and TRAP-MVNP OCL precursors were immunoprecipitated with an antibody against ATF7 or TAF12, and the immune complexes were analyzed by Western blot with anti-TAF12 and anti-ATF7, respectively. **(C)** VDR content of ATF7 contribute by 1,25-(OH)<sub>2</sub>D<sub>3</sub>. OCL precursor cells from TRAP-MVNP which transduced ATF7 or control shRNA were cultured for 24 or 48 hours on 10<sup>-8</sup>M 1,25-(OH)<sub>2</sub>D<sub>3</sub> and amounts of VDR were quantified by Western blot. **(D)** The role of ATF7 on OCL formation. ATF7 shRNA was transduced into MVNP and WT OCL precursors as describe in material and methods, the cells cultured for 7 days with 1,25-(OH)<sub>2</sub>D<sub>3</sub>, then cells were stained for TRAP. Cells

with 3 or more nuclei were scored as OCL. Results are expressed as mean  $\pm$  SD (n=4). \*; Significantly different from OCL formed with the same treatment in WT mouse cultures.  $p < 0.01$ .

**Figure 2. ChIP assay demonstrating that TAF12 binds at the CYP24A1 promoter in OCL precursors from TRAP-MVNP and WT mice:** (A) CD11b(+) marrow mononuclear cells from wild type and TRAP-MVNP mice ( $1 \times 10^7$  cells) were cultured with  $1,25-(OH)_2D_3$  ( $10^{-8}M$ ) for 24 hours and then subjected to ChIP analysis. ChIP assays were performed using anti-TAF12 (Protein Tech Group) or anti-IgG (Santa Cruz) for control. The mouse *CYP24A1* specific primers were 5'-AAG GAC ACA GAG GAA GAA GCC-3' (sense), 5'- GAA TGG CAC ACT TGG GGT AAG-3' (antisense). (B) Loss of ATF7 decreases TAF12 binding to the *CYP24A1* promoter CD11b(+) marrow mononuclear cells from wild type and TRAP-MVNP mice were transduced with *ATF7*shRNA and cultured with  $1,25-(OH)_2D_3$  ( $10^{-8}M$ ) for 24 hours and then subjected to ChIP analysis. ChIP assays were performed using an antibody anti-TAF12 (Protein Tech Group) or anti-IgG (Santa Cruz) for control. The mouse *CYP24A1* specific primers were 5'-AAG GAC ACA GAG GAA GAA GCC-3' (sense), 5'- GAA TGG CAC ACT TGG GGT AAG-3' (antisense).

#### 4. KEY RESEARCH ACOMPLISHMENTS:

- Immunoprecipitation of lysates from either WT or *MVNP*-expressing OCL with an anti-TAF12 antibody followed by blotting with an anti-ATF7 antibody, or vice versa, showed that TAF12 and ATF7 physically interact in OCL.
- ChIP analysis of OCL precursors using an anti-TAF12 antibody demonstrated that TAF12 binds the 24-hydroxylase (*CYP24A1*) promoter, which contains two functional vitamin D response elements (VDRE), in the presence of  $1,25-(OH)_2D_3$ .
- TAF12 is a functional partner of ATF7 in OCL formation by  $1,25-(OH)_2D_3$ .
- Knockdown of ATF7 in *MVNP*-expressing cells decreased *CYP24A1* induction by  $1,25-(OH)_2D_3$  as well as TAF12 binding to the *CYP24A1* promoter.

#### 5. CONCLUSION:

ATF7 and TAF12 are required for  $1,25-(OH)_2D_3$  hyper-sensitivity of OCL precursors.

To determine the role of TAF12 in normal and pagetic OCL activity in vivo, we are developing TAF12 knockout mice and TRAP-cre/TAF12<sup>-/-</sup> mice (Task 3A).

#### 6. PUBLICATIONS, ABSTRACTS AND PRESENTATIONS:

Publication;

- (1) Teramachi J, Hiruma Y, Ishizuka S, Ishizuka H, Brown JP, Michou L, Cao H, Galson DL, Subler MA, Zhou H, Dempster DW, Windle JJ, Roodman GD, Kurihara N. Role of ATF7-TAF12 interactions in the vitamin D response hypersensitivity of osteoclast precursors in Paget's disease. J Bone Miner Res. 2013; 28(6):1489
- (2) Teramachi J, Zhou H, Subler MA, Kitagawa Y, Galson DL, Dempster DW, Windle JJ, Kurihara N, Roodman GD Increased IL-6 Expression in Osteoclasts is Necessary but not Sufficient for the Development of Paget's Disease of Bone. J Bone Miner Res. 2013 (in press).

Abstract: None

Presentation: None

**7. INVENTION, PATENTS AND LICENCES:** None

**8. REPORTABLE OUTCOMES:** TAF12 induced by MVNP is not required for development of PD, but is required for development of 1,25-(OH)<sub>2</sub>D<sub>3</sub> hyper-responsivity of PD osteoclast precursors.

**9. OTHER ACHIVEMENT:** None

## **10. REFERENCES**

- (1) Krötz F, de Wit C, Sohn HY, Zahler S, Gloe T, Pohl U, Plank C. Magnetofection--a highly efficient tool for antisense oligonucleotide delivery in vitro and in vivo. Mol Ther. 2003;7:700-710.
- (2) Hofmann A, Wenzel D, Becher UM, Freitag DF, Klein AM, Eberbeck D, Schulte M, Zimmermann K, Bergemann C, Gleich B, Roell W, Weyh T, Trahms L, Nickenig G, Fleischmann BK, Pfeifer A. Combined targeting of lentiviral vectors and positioning of transduced cells by magnetic nanoparticles. Proc Natl Acad Sci U S A. 2009;106(1):44-9
- (3) Yu S, Franceschi RT, Luo M, Fan J, Jiang D, Cao H, Kwon TG, Lai Y, Zhang J, Patrene K, Hankenson K, Roodman GD, Xiao G. Critical role of activating transcription factor 4 in the anabolic actions of parathyroid hormone in bone. PLoS One. 2009 ;4:e7583.
- (4) Yu S, Jiang Y, Galson DL, Luo M, Lai Y, Lu Y, Ouyang HJ, Zhang J, Xiao G. General transcription factor IIA-gamma increases osteoblast-specific osteocalcin gene expression via activating transcription factor 4 and runt-related transcription factor 2. J Biol Chem. 2008 ;283:5542-5553.

## **11. APPENDICES:**

- (1) J Bone Miner Res. 2013; 28(6):1489 (PDF file)
- (2) J Bone Miner Res. 2013; Dec. 11 (PDF file)
- (3) Figures 1 and 2

# Role of ATF7-TAF12 Interactions in the Vitamin D Response Hypersensitivity of Osteoclast Precursors in Paget's Disease

Jumpei Teramachi,<sup>1</sup> Yuko Hiruma,<sup>2</sup> Seiichi Ishizuka,<sup>2</sup> Hisako Ishizuka,<sup>2</sup> Jacques P Brown,<sup>3</sup> Laëtitia Michou,<sup>3</sup> Huiling Cao,<sup>2</sup> Deborah L Galson,<sup>2</sup> Mark A Subler,<sup>4</sup> Hua Zhou,<sup>5</sup> David W Dempster,<sup>5</sup> Jolene J Windle,<sup>4</sup> G David Roodman,<sup>1</sup> and Noriyoshi Kurihara<sup>1</sup>

<sup>1</sup>Department of Medicine, Hematology Oncology, Indiana University, Indianapolis, IN, USA

<sup>2</sup>Department of Medicine, Hematology Oncology, University of Pittsburgh and the Center for Bone Biology at University of Pittsburgh Medical Center, Pittsburgh, PA, USA

<sup>3</sup>Laval University, CHUQ-CHUL Research Centre, Quebec, QC, Canada

<sup>4</sup>Department of Human and Molecular Genetics, Virginia Commonwealth University, Richmond, VA, USA

<sup>5</sup>Department of Pathology, College of Physician and Surgeons, Columbia University, New York, NY, USA

## ABSTRACT

Osteoclast (OCL) precursors from many Paget's disease (PD) patients express measles virus nucleocapsid protein (MVNP) and are hypersensitive to 1,25-dihydroxyvitamin D<sub>3</sub> (1,25-(OH)<sub>2</sub>D<sub>3</sub>; also known as calcitriol). The increased 1,25-(OH)<sub>2</sub>D<sub>3</sub> sensitivity is mediated by transcription initiation factor TFIID subunit 12 (TAF12), a coactivator of the vitamin D receptor (VDR), which is present at much higher levels in MVNP-expressing OCL precursors than normals. These results suggest that TAF12 plays an important role in the abnormal OCL activity in PD. However, the molecular mechanisms underlying both 1,25-(OH)<sub>2</sub>D<sub>3</sub>'s effects on OCL formation and the contribution of TAF12 to these effects in both normals and PD patients are unclear. Inhibition of TAF12 with a specific *TAF12* antisense construct decreased OCL formation and OCL precursors' sensitivity to 1,25-(OH)<sub>2</sub>D<sub>3</sub> in PD patient bone marrow samples. Further, OCL precursors from transgenic mice in which *TAF12* expression was targeted to the OCL lineage (tartrate-resistant acid phosphatase [TRAP]-*TAF12* mice), formed OCLs at very low levels of 1,25-(OH)<sub>2</sub>D<sub>3</sub>, although the OCLs failed to exhibit other hallmarks of PD OCLs, including receptor activator of NF-κB ligand (RANKL) hypersensitivity and hypermultinucleation. Chromatin immunoprecipitation (ChIP) analysis of OCL precursors using an anti-TAF12 antibody demonstrated that TAF12 binds the 24-hydroxylase (*CYP24A1*) promoter, which contains two functional vitamin D response elements (VDREs), in the presence of 1,25-(OH)<sub>2</sub>D<sub>3</sub>. Because TAF12 directly interacts with the cyclic adenosine monophosphate-dependent activating transcription factor 7 (ATF7) and potentiates ATF7-induced transcriptional activation of ATF7-driven genes in other cell types, we determined whether TAF12 is a functional partner of ATF7 in OCL precursors. Immunoprecipitation of lysates from either wild-type (WT) or *MVNP*-expressing OCL with an anti-TAF12 antibody, followed by blotting with an anti-ATF7 antibody, or vice versa, showed that TAF12 and ATF7 physically interact in OCLs. Knockdown of *ATF7* in *MVNP*-expressing cells decreased cytochrome P450, family 24, subfamily A, polypeptide 1 (*CYP24A1*) induction by 1,25-(OH)<sub>2</sub>D<sub>3</sub>, as well as TAF12 binding to the *CYP24A1* promoter. These results show that ATF7 interacts with TAF12 and contributes to the hypersensitivity of OCL precursors to 1,25-(OH)<sub>2</sub>D<sub>3</sub> in PD. © 2013 American Society for Bone and Mineral Research.

**KEY WORDS:** TAF12; VITAMIN D; PAGET'S DISEASE; OSTEOCLASTS; ATF7

## Introduction

Paget's disease (PD) is a very common bone disease that affects 1 million to 2 million Americans. It is one of the most exaggerated forms of coupled bone remodeling, in which excessive bone resorption is followed by exuberant bone formation, and it provides important insights into the normal

bone remodeling process.<sup>(1,2)</sup> Studies of PD have revealed that 1,25-dihydroxyvitamin D<sub>3</sub> (1,25-(OH)<sub>2</sub>D<sub>3</sub>; also known as calcitriol) can act directly on osteoclast (OCL) precursors to induce OCL formation independent of receptor activator of NF-κB ligand (RANKL), and that osteoclast (OCL) precursors from PD patients form OCLs at physiologic ( $1 \times 10^{-11}$  M) rather than the pharmacologic ( $1 \times 10^{-8}$  M) concentrations of 1,25-(OH)<sub>2</sub>D<sub>3</sub>

Received in original form September 10, 2012; revised form January 7, 2013; accepted January 21, 2013. Accepted manuscript online February 20, 2013.

Address correspondence to: Noriyoshi Kurihara, DDS, PhD, Indiana University, Hematology Oncology, 980 W Walnut St., Indianapolis, IN 46202, USA.

E-mail: norikuri@iupui.edu

Journal of Bone and Mineral Research, Vol. 28, No. 6, June 2013, pp 1489–1500

DOI: 10.1002/jbmr.1884

© 2013 American Society for Bone and Mineral Research

required for normal OCL precursors.<sup>(3)</sup> This enhanced sensitivity on OCL precursors to 1,25-(OH)<sub>2</sub>D<sub>3</sub> in PD results from increased expression of transcription initiation factor TFIID subunit 12 (TAF12; formerly TAF<sub>II</sub>-17), a member of the TFIID transcription factor complex.<sup>(4–6)</sup> TAF12 acts as a coactivator of the vitamin D receptor (VDR), and increased levels of TAF12 enhance the VDR responsiveness of OCL precursors from PD patients.<sup>(7)</sup> However, the molecular mechanisms regulating TAF12's effects on genes activated by 1,25-(OH)<sub>2</sub>D<sub>3</sub>/VDR in OCLs are undefined.

We and others have previously shown that both environmental factors, in particular measles virus, and genetic factors, such as mutant p62/sequestosome 1 (eg, p62<sup>P392L</sup>), both contribute to the pathogenesis of PD.<sup>(8–10)</sup> However, genetic factors alone do not appear to be sufficient to induce PD. We reported that transfection of the p62<sup>P392L</sup> gene into normal OCL precursors does not result in formation of pagetic-like OCLs in vitro. Importantly, OCLs from transgenic mice overexpressing the p62<sup>P392L</sup> mutation or p62<sup>P394L</sup> knock-in mice do not express elevated TAF12, are not hypersensitive to 1,25-(OH)<sub>2</sub>D<sub>3</sub>, and in our experience do not develop pagetic bone lesions.<sup>(11)</sup>

In contrast, transfection of normal OCL precursors with the measles virus nucleocapsid protein (MVNP) gene results in development of OCLs that exhibit most of the characteristics of PD OCLs, including increased TAF12 expression and VDR hypersensitivity in OCL precursors as well as other cell types.<sup>(8)</sup> Further, targeting MVNP to the OCL lineage in transgenic mice (tartrate-resistant acid phosphatase [TRAP]-MVNP mice) induces formation of bone lesions and OCL characteristic of PD.<sup>(10)</sup> Thus, TRAP-MVNP mice provide us an in vivo model to further explore the molecular mechanisms responsible for vitamin D<sub>3</sub>'s effects on OCL formation and activity in PD as well as in normal bone remodeling. We recently showed that blocking MVNP expression in MVNP-positive OCLs from PD patients using an antisense construct resulted in loss of the pagetic phenotype and reduced TAF12 expression, regardless of whether the OCLs also harbored a p62 mutation.<sup>(8)</sup> However, the role that TAF12 and 1,25-(OH)<sub>2</sub>D<sub>3</sub> hypersensitivity play in the development of the "pagetic phenotype" in OCL and PD is still unclear.

Previous studies showed that TAF12 levels were increased in colorectal cancer cells harboring a RAS mutation, and that TAF12 levels were reduced when the cells were treated with a mitogen-activated protein kinase kinase inhibitor (MEK).<sup>(12)</sup> Further, TAF12 overexpression was found to potentiate cyclic adenosine monophosphate-dependent activating transcription factor 7 (ATF7)-induced transcriptional activation through direct interaction in colorectal cancer cells, and this effect was inhibited by TAF4, which blocks the interaction between TAF12 and ATF7.<sup>(13)</sup>

Therefore, we examined the role of TAF12 and ATF7 in VDR-mediated OCL formation, using both human colony-forming unit-granulocyte macrophage (CFU-GM; a highly purified population of early-osteoclast precursors) transduced with a TAF12 retrovirus, and OCL precursors from transgenic mice with TAF12 expression targeted to the OCL. We found that ATF7 physically interacts with TAF12 and increases TAF12 levels in OCL precursors, contributes to the 1,25-(OH)<sub>2</sub>D<sub>3</sub> hypersensitivity of OCL precursors induced by TAF12, and that OCL from TRAP-TAF12 mice were hypersensitive to 1,25-(OH)<sub>2</sub>D<sub>3</sub> and produced increased levels of interleukin 6 (IL-6) compared to wild-type

(WT) mice. However, increased expression of TAF12 by itself was not sufficient to induce hypermultinucleated OCL or pagetic bone lesions, demonstrating that other factors in addition to increased TAF12 expression are required to induce pagetic OCLs and bone lesions.

## Materials and Methods

OCL formation by PD and normal OCL precursors transduced with antisense (AS)-TAF12 or scrambled antisense to TAF12.

Human marrow mononuclear cells isolated from involved sites of 3 MVNP<sup>+</sup> Paget's patients and 2 normals were cultured for 96 hours with cytokines and the retroviral supernatants as described.<sup>(8)</sup> These studies were approved by the Institutional Review Board at the University of Pittsburgh. The cells were resuspended at  $2.5 \times 10^6$  cells/mL and were cultured in  $\alpha$ -Minimal Essential Medium ( $\alpha$ -MEM; Gibco BRL Invitrogen, Carlsbad, CA, USA) containing 10% fetal bovine serum (FBS; Invitrogen) plus 10 ng/mL each of IL-3, IL-6, and stem cell growth factor for 2 days to induce proliferation of hematopoietic precursors. The marrow cells were then transduced with retroviral vectors that contained a neomycin resistance gene and the human AS-TAF12 (cytomegalovirus promoter [pCMV]/AS-TAF12) or scrambled antisense TAF12 (pCMV/scrambled AS-TAF12). The transduced cells were cultured in methylcellulose with human GM-colony-stimulating factor (GM-CSF) (200 pg/mL) in the presence of 250 pg/mL Geneticin (G418; Sigma-Aldrich, St. Louis, MO, USA) to select for CFU-GM colonies that expressed AS-TAF12 or scrambled AS-TAF12. CFU-GM colony-derived cells that expressed AS-TAF12 or scrambled AS-TAF12 ( $2 \times 10^5$  cells/well, 96-well plate) were cultured in  $\alpha$ -MEM + 20% horse serum for 21 days in the presence of varying concentrations of 1,25-(OH)<sub>2</sub>D<sub>3</sub>. Cells were then stained for 23C6 (CD51) using a Vectastain kit (Vector Laboratory, Burlingame, CA, USA), and 23C6<sup>+</sup> multinucleated cells ( $\geq 3$  nuclear/cells) were counted as OCLs.<sup>(8)</sup>

### OCL formation by normal human OCL precursors transduced with the TAF12 gene or empty vector

Nonadherent mononuclear human marrow cells were collected by bone marrow aspiration from normal volunteers as described.<sup>(8)</sup> These studies were approved by the Institutional Review Board at the University of Pittsburgh. The cells were resuspended at  $2.5 \times 10^6$  cells/mL and were cultured in  $\alpha$ -MEM containing 10% FBS plus 10 ng/mL each of IL-3, IL-6, and stem cell growth factor for 2 days to induce proliferation of hematopoietic precursors. The marrow cells were then transduced with retroviral vectors that contained a neomycin resistance gene and the human TAF12 cDNA (pCMV/TAF12), MVNP (pCMV/MVNP) or empty vector (EV).<sup>(9,14)</sup> The transduced cells were cultured for OCL formation as described above.<sup>(14)</sup>

### Development of TRAP-TAF12 transgenic mice

All studies were approved by the Institutional Animal Care and Use Committees (IACUCs) at both the University of Pittsburgh School of Medicine and Virginia Commonwealth University. To generate the TRAP-TAF12 transgene construct, a 0.5-kb human

*TAF12* cDNA (originally derived from a Paget's patient) was inserted into the unique *EcoRI* site of the promoter 3-ketoacyl-coenzyme A reductase (pKCR3)-modified TRAP (mTRAP) vector.<sup>(15,16)</sup> pKCR3-mTRAP contains 1.9 kb of the mouse TRAP gene promoter and 5'-untranslated region (5'-UTR), in addition to rabbit  $\beta$ -globin intron 2 and its flanking exons (for efficient transgene expression). A 3.6-kb injection fragment was then excised from the TRAP-*TAF12* construct with *XhoI*, and transgenic mice were generated by standard methods in a CB6F1 (C57Bl/6  $\times$  Balb/c) genetic background.<sup>(17)</sup> Potential founders were screened for the presence of the TRAP-*TAF12* transgene by PCR analysis of genomic tail DNA using a mouse TRAP sense primer (5'-CTGGACAATCCTCGGAGAAAATGC-3') and a rabbit  $\beta$ -globin antisense primer (5'-GCGAAAAAGAAACAATCAAG-3'). Amplification of DNA from mice carrying the TRAP-*TAF12* transgene generated a 591-bp PCR product. Founders were bred to establish multiple independent lines of mice. To verify the integrity of the TRAP-*TAF12* transgene, Southern blot analysis of DNA from founders and their progeny was performed using the *XhoI* injection fragment as probe.

### Osteoclast formation from transgenic mouse bone marrow

Bone marrow cells were flushed from long bones of WT, TRAP-*TAF12*, or TRAP-MVNP<sup>(10)</sup> mice of various ages and plated on 100-mm tissue culture plates in  $\alpha$ -MEM containing 10% FBS. Cells were incubated at 37°C in 5% CO<sub>2</sub> overnight. Nonadherent cells were harvested and enriched for CD11b<sup>+</sup> mononuclear cells using the Miltenyi Biotec MACS (Magnetic Cell Sorting) system.<sup>(7)</sup> CD11b<sup>+</sup> cells then were cultured in  $\alpha$ -MEM containing 10% FBS plus 10 ng/mL of macrophage colony-stimulating factor (M-CSF; R&D, Systems, Minneapolis, MN, USA) for 3 days to generate a population of enriched early OCL precursors. These were then cultured in  $\alpha$ -MEM containing 10% FBS in the presence of 1,25-(OH)<sub>2</sub>D<sub>3</sub> (Teijin Pharma, Tokyo, Japan) for 3 to 4 days to generate OCLs, and cells were then stained for TRAP using a leukocyte acid phosphatase kit (Sigma), TRAP-positive cells ( $\geq 3$  nuclei/cell) were scored microscopically.

### Bone resorption assays of cultured OCLs

CD11b<sup>+</sup> cells were cultured on mammoth dentin slices (Wako, Osaka, Japan) in  $\alpha$ -MEM containing 10% FCS and 1,25-(OH)<sub>2</sub>D<sub>3</sub> ( $1 \times 10^{-8}$  M). After 14 days of culture, the cells were removed, the dentin slices were stained with acid hematoxylin, and the areas of dentin resorption were determined using image-analysis techniques (NIH Image System).<sup>(8)</sup>

### Chromatin immunoprecipitation assays

Chromatin immunoprecipitation (ChIP) assays were performed as described,<sup>(18,19)</sup> using osteoclast precursors from TRAP-MVNP or WT mice. The equivalent of 10  $\mu$ g DNA was used as starting material (input) in each ChIP reaction. The DNA was fragmented by sonication and then immunoprecipitated with 2  $\mu$ g of anti-TAF12 antibody (Protein Tech Group, Inc., St. Louis, MO, USA). Portions of the ChIP DNA fractions (5%) or starting DNA (0.02% to 0.05%) were used for PCR analysis. The reaction was performed

with AmpliTaq Gold DNA Polymerase (Invitrogen, Carlsbad, CA, USA) for 35 cycles of 60 seconds at 95°C, 90 seconds at 58°C, and 120 seconds at 68°C. The gene-specific primers for mouse *CYP24A1* mRNA were 5'-ATT ACC TGA GAA TCA GAG GCC ACG-3' (sense) and 5'-GCC AAA TGC AGT TTA AGC TCT GCT-3' (antisense). The PCR products were separated on 2% agarose gels and visualized with ultraviolet light. All ChIP assays were repeated at least three times.

### Quantitative reverse-transcription PCR analysis

CD11b<sup>+</sup> cells from human bone marrow were cultured with 1,25-(OH)<sub>2</sub>D<sub>3</sub> or vehicle for 2 days and subjected to reverse-transcription PCR (RT-PCR) analysis for expression of *CYP24A1* mRNA. Total RNA was extracted using RNeasy Lysis solution (Qiagen, Crawfordsville, IN, USA) and cDNAs were synthesized using an RNA PCR Kit (Applied Biosystems, Foster City, CA, USA). The gene-specific primers for mouse *CYP24A1* mRNA were 5'-ATT ACC TGA GAA TCA GAG GCC ACG-3' (sense) and 5'-GCC AAA TGC AGT TTA AGC TCT GCT-3' (antisense). The gene-specific primers for mouse  $\beta$ -actin were 5'-GGC CGT ACC ACT GGC ATC GTG ATG-3' (sense) and 5'-CTT GGC CGT CAG GCA GCT CGT AGC-3' (antisense).

### Immunoblotting of OCL precursor lysates from WT, TRAP-MVNP, or TRAP-TAF12 mice

OCL precursors from WT, TRAP-MVNP, or TRAP-*TAF12* mice were washed twice with ice-cold phosphate buffered saline (PBS), and were then lysed in buffer containing 20 mM Tris, pH 7.5, 150 mM NaCl, 1 mM ethylenediaminetetraacetic acid (EDTA), 1 mM ethylene glycol-bis-(2-aminoethyl)-N,N,N', N'-tetraacetic acid (EGTA), 1% Triton X-100, 2.5 mM sodium pyrophosphate, 1 mM  $\beta$ -glycerophosphate, 1 mM Na<sub>3</sub>VO<sub>4</sub>, 1 mM NaF, and  $\times 1$  protease inhibitor mixture. Cell lysates (50  $\mu$ g) were boiled in the presence of sodium dodecyl sulfate (SDS) sample buffer (0.5 M Tris-HCl, pH 6.8, 10% wt/vol SDS, 10% glycerol, 0.05% wt/vol bromophenol blue) for 5 minutes and subjected to electrophoresis on 4% to 20% SDS-PAGE (Bio-Rad Laboratories, Hercules, CA, USA). Proteins were transferred to nitrocellulose membranes using a semidry blotter (Bio-Rad) and incubated in blocking solution (5% nonfat dry milk in TBS containing 0.1% Tween-20) for 1 hour to reduce nonspecific binding. Membranes were then exposed to primary antibodies overnight at 4°C, washed three times, and incubated with secondary goat anti-mouse or rabbit immunoglobulin G (IgG) horseradish peroxidase (HRP)-conjugated antibody for 1 hour. Membranes were washed extensively, and an enhanced chemiluminescence detection assay was performed following the manufacturer's directions (Bio-Rad). All blots were densitometrically quantitated and the results expressed relative to control and normalized to  $\beta$ -actin or TFIIIB (Santa Cruz Biotechnology Inc., Santa Cruz, CA, USA).

### IL-6 ELISA assay

Conditioned media from mouse OCL cultures was harvested 7 days after the addition of 1,25-(OH)<sub>2</sub>D<sub>3</sub>. The concentration of IL-6 present was determined using an ELISA kit for mouse IL-6 (R&D), according to the manufacturer's instructions and were normalized to cell number.

## ATF7 short-hairpin RNA transduction

Nonadherent bone marrow cells from TRAP-MVNP and WT mice were transduced with ATF7 short-hairpin RNA (shRNA) (NM\_146065) (Sigma-Aldrich) or control shRNA (Sigma-Aldrich) that were designed by MISSION. The shRNA Lentiviral transduction particles (Sigma-Aldrich) were used for transduction. The transduction was performed by the MagnetoFection-ViroMag R/L methods (OZ Biosciences, Marseille, France) according to the manufacturer's instructions.<sup>(20,21)</sup> To increase the transduction efficiency, the cells were plated the day before transduction in 96-well culture plates in the presence of 10 ng/mL of macrophage colony-stimulating factor (M-CSF) and 2  $\mu$ L of ViroMag R/L beads in 50  $\mu$ L of  $\alpha$ -MEM 10% FCS containing 10 ng/mL of M-CSF, then 500 multiplicity of infection (MOI) of Lentiviral transduction particles were added, and the cells were incubated for 15 minutes at room temperature. Then 50  $\mu$ L of virus particles/magnet were mixed in each well and cells were incubated on a magnet plate for 60 minutes. The culture plates were removed from the magnetic plate and cells were cultured with or with 1,25-(OH)<sub>2</sub>D<sub>3</sub> ( $1 \times 10^{-8}$  M) for 7 days. The level of OCL formation was determined by counting the number of TRAP<sup>+</sup> multinucleated cells ( $\geq 3$  nuclei/cell).

## Quantitative micro-computed tomography measurements

The gross morphologic and microarchitectural traits of the distal area of the femur and L<sub>5</sub> vertebra were examined by quantitative micro-computed tomography ( $\mu$ CT). The L<sub>5</sub> vertebrae were used to assess histomorphometry of the trabecular bones, and the femurs were used to measure mean cortical thickness. Specimens were held with Styrofoam within plastic vials and positioned within a 25-mm-diameter acrylic tube. After an initial scout scan, full-length scans were obtained at an isotropic voxel resolution of 10.5  $\mu$ m using a commercial scanner (Scanco Viva CT40; Scanco Medical AG, Bassersdorf, Switzerland) using the following settings: energy = 55 kVp, current = 145 mA, and integration time = 300 ms. A total of 300 slices with an increment of 25  $\mu$ m were obtained on each bone sample starting 1.0 mm below the growth plate in the area of the secondary spongiosa. The area for analysis was outlined within the trabecular compartment, excluding the cortical and subcortical bone. Every 25 sections were outlined, and the intermediate sections were interpolated with the contouring algorithm to create a volume of interest. Segmentation values used for analysis were sigma 0.8, support 1, and threshold 275. A three-dimensional (3D) analysis was done to determine bone volume fraction (BV/TV, %), trabecular number (Tb.N, N/ $\mu$ m<sup>2</sup>), trabecular thickness (Tb.Th,  $\mu$ m), and trabecular bone spacing (Tb.Sp,  $\mu$ m). Cortical bone also was analyzed in the femur 2 mm below the growth plate, and the same segmentation parameters were used for analysis.

## Bone histomorphometric analyses

Mice were given calcein (10 mg/kg) on day -7 and day -2 prior to euthanasia. Lumbar vertebrae from 13 TRAP-TAF12 transgenic mice and 24 WT mice were subjected to qualitative histological examination and quantitative histomorphometry. The bones were fixed in 10% buffered formalin at 4°C. The first four lumbar

vertebrae (L<sub>1</sub>–L<sub>4</sub>) were decalcified in 10% EDTA at 4°C and embedded in paraffin. L<sub>5</sub> was embedded without decalcification in methyl methacrylate. Five-micrometer (5- $\mu$ m) frontal sections were cut for both decalcified and undecalcified samples. The decalcified sections were stained for TRAP, and OCL containing active TRAP were stained red as described by Liu and colleagues.<sup>(22)</sup> The undecalcified sections were left unstained for the evaluation of fluorescent labels.

All sections were first evaluated qualitatively by microscopy to detect any unusual lesions, and were then analyzed by histomorphometry. The analysis was performed on the cancellous bone/marrow compartment between the cranial and caudal growth plates in the vertebral bodies without lesions using the OsteoMeasure XPTM version 1.01 morphometric program (OsteoMetrics, Inc., Atlanta, GA, USA). Osteoclast perimeter (Oc.Pm)—defined as the length of bone surface covered with TRAP-positive mononuclear and multinuclear cells—and cancellous BV/TV, trabecular width (Tb.Wi), Tb.N, Tb.Sp, mineralizing perimeter (Md.Pm), mineral apposition rate (MAR), and bone formation (BFR) were quantified and calculated. All variables were calculated and expressed and calculated according to the recommendations of the ASBMR Nomenclature Committee.<sup>(23)</sup>

## Statistical analysis

For all cell culture studies, significance was evaluated using a two-tailed unpaired Student's *t* test, with *p* < 0.05 considered to be significant.

## Results

### Effects of antisense to TAF12 on OCL formation in marrow cultures from PD patients that carry the *p62*<sup>P392L</sup> mutation and express MVNP in their OCL precursors

We previously reported that expression of TAF12 was higher in OCL precursors from PD patients than from normals,<sup>(7,8)</sup> and that OCL precursors from PD patients that carried the *p62*<sup>P392L</sup> mutation linked to PD and also expressed MVNP were hyperresponsive to 1,25-(OH)<sub>2</sub>D<sub>3</sub> and expressed increased levels of TAF12.<sup>(8)</sup> Therefore, to determine the contribution of TAF12 to the hypersensitivity to 1,25-(OH)<sub>2</sub>D<sub>3</sub>, we transduced a retrovirus construct containing an antisense to TAF12 into MVNP<sup>+</sup> OCL precursors from PD patients and normal OCL precursors. The TAF12 antisense construct decreased TAF12 expression by more than 80% (data not shown) and the 1,25-(OH)<sub>2</sub>D<sub>3</sub> hypersensitivity of the PD OCL precursors (Fig. 1), similar to the effects of antisense MVNP. The TAF12 antisense construct had no effect on 1,25-(OH)<sub>2</sub>D<sub>3</sub> sensitivity in normal marrow cultures.

### Overexpression of TAF12 in human CFU-GM is sufficient to enhance 1,25-(OH)<sub>2</sub>D<sub>3</sub> hypersensitivity

We then examined the effects of overexpression of TAF12 in normal OCL precursors. These experiments allowed a direct assessment of the capacity of increased levels of TAF12 to mediate 1,25-(OH)<sub>2</sub>D<sub>3</sub> hypersensitivity in OCL precursors in vitro and to determine the potential of TAF12 in the development of pagetic OCL.

The cDNA for TAF12 was synthesized by RT-PCR from OCL precursor cells of PD patients and inserted into a retroviral

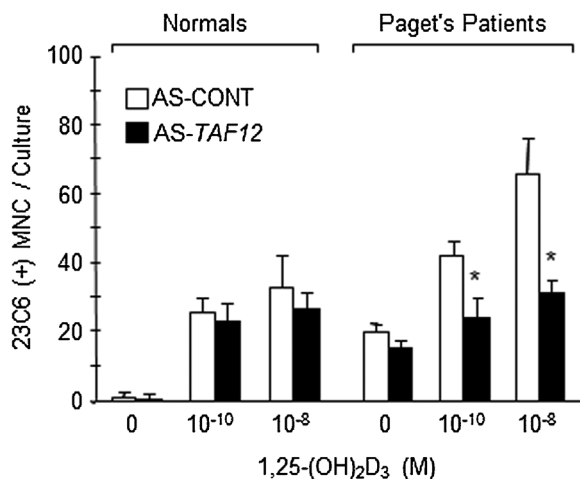


**Fig. 1.** OCL formation stimulated by 1,25-(OH)<sub>2</sub>D<sub>3</sub> is reduced in antisense TAF12-transduced human OCL precursors from PD patients but not from normals. AS-TAF12 or scrambled antisense-transduced OCL precursor cells from 3 PD patients or 2 normals were cultured in methylcellulose with recombinant GM-CSF and G418. G418-resistant CFU-GM-derived CD11b<sup>+</sup> cells were then cultured with varying concentrations of 1,25-(OH)<sub>2</sub>D<sub>3</sub> for 3 weeks. The cells were then fixed and stained with the 23C6 monoclonal antibody, which identifies OCLs. The results represent the mean  $\pm$  SD of aggregate data from 3 MVNP<sup>+</sup> patients and 2 normals. \**p* < 0.01 compared to scrambled antisense transduced cells.

construct as described.<sup>(7)</sup> Either TAF12-transduced or MVNP-expressing virus was transduced into normal human marrow cells and OCL precursors treated with varying concentrations of 1,25-(OH)<sub>2</sub>D<sub>3</sub>, and the number and characteristics of the OCL formed were determined. Both MVNP-transduced and TAF12-transduced normal OCL precursors demonstrated about a twofold increase of TAF12 mRNA expression levels (not shown). In addition, both expressed increased levels of CYP24A1 mRNA compared to EV-transduced OCL precursors when treated with 1  $\times$  10<sup>-11</sup> to 1  $\times$  10<sup>-7</sup> 1,25-(OH)<sub>2</sub>D<sub>3</sub> (Fig. 2A). TAF12-transduced cells formed increased numbers of OCL that were hypersensitive to 1,25-(OH)<sub>2</sub>D<sub>3</sub> (Fig. 2B, C), but in contrast to MVNP-expressing cells, did not contain increased numbers of nuclei per OCL at low levels of 1,25-(OH)<sub>2</sub>D<sub>3</sub> (Fig. 2B, C) or produce high levels of IL-6 (47  $\pm$  1 pg/mL versus 269  $\pm$  11 pg/mL, TAF12-transduced versus MVNP-transduced cells). The EV-transduced cells did not produce detectable levels of IL-6 (<5 pg/mL).

We then determined the bone resorbing capacity of TAF12-transduced OCL precursors treated with 1,25-(OH)<sub>2</sub>D<sub>3</sub>. OCL formed by MVNP-transduced OCL precursors treated with 1,25-(OH)<sub>2</sub>D<sub>3</sub> had a markedly increased bone-resorbing capacity per OCL, whereas the bone resorption capacity per OCL formed by TAF12-transduced OCL precursors was similar to those from EV-transduced OCL precursors (Fig. 2D).

#### Osteoclast precursors from TRAP-TAF12 mice display 1,25-(OH)<sub>2</sub>D<sub>3</sub> hypersensitivity

We generated TRAP-TAF12 transgenic mice in which TAF12 expression is targeted to the OCL lineage with the TRAP promoter. Four founder mice were obtained, and lines of mice were generated from each. Levels of TAF12 expression in OCL

precursors were measured by Western blot, and two lines expressing TAF12 comparable to the levels seen in TRAP-MVNP mice were selected for further analysis (Fig. 3A). Comparable results were obtained from mice of both lines, and all of the results shown here were obtained from mice of line 2. When bone marrow from TRAP-TAF12 and TRAP-MVNP mice was cultured with 1,25-(OH)<sub>2</sub>D<sub>3</sub> or RANKL, OCLs were formed at low concentrations (1  $\times$  10<sup>-10</sup>M) of 1,25-(OH)<sub>2</sub>D<sub>3</sub> in both lines, a concentration that does not induce OCL formation in marrow from WT mice (Fig. 3B), but neither line was hyperresponsive to RANKL. OCL formed from TRAP-MVNP marrow exhibited markedly elevated nuclear numbers per OCL in response to 1,25-(OH)<sub>2</sub>D<sub>3</sub>, but the nuclear numbers per OCL in TRAP-TAF12 mice were similar to WT OCLs (Fig. 3C). To determine if these OCL precursors demonstrated enhanced VDR-mediated transcription at low concentrations of 1,25-(OH)<sub>2</sub>D<sub>3</sub>, the expression of CYP24A1 (a classic 1,25-(OH)<sub>2</sub>D<sub>3</sub>-responsive gene with two vitamin D response elements [VDREs] in its promoter) was measured. As shown in Fig. 3D, OCL precursors from both TRAP-MVNP and TRAP-TAF12 mice showed increased CYP24A1 expression compared to WT mice when treated with low concentrations of 1,25-(OH)<sub>2</sub>D<sub>3</sub>. IL-6 production following 1,25-(OH)<sub>2</sub>D<sub>3</sub> treatment was also increased in OCL precursors from both TRAP-MVNP and TRAP-TAF12 mice compared to WT mice, but to a lesser extent in the TRAP-TAF12 OCLs (Fig. 3E).

#### Bone phenotype of TRAP-TAF12 mice

We examined the bone phenotype of TRAP-TAF12 mice at 12 months of age in the lumbar vertebral bodies by qualitative histology and histomorphometry, and in the femur and L<sub>5</sub> vertebra by  $\mu$ CT. The histomorphometry studies showed that no pagetic lesions were found in the lumbar vertebral bone of the TRAP-TAF12 or WT mice. There were no significant differences between the TRAP-TAF12 and the WT mice in bone structural variables of cancellous BV/TV, Tb.N, Tb.Wi, Tb.Sp, nor in the Oc.Pm, Md.Pm, MAR, and BFR (Fig. 4). The result of  $\mu$ CT analysis of the femur and L<sub>5</sub> vertebra revealed no significant differences (Fig. 4).

#### TAF12 binds the CYP24A1 promoter

ChIP analysis was performed using an anti-TAF12 antibody and primers flanking the two VDREs in the CYP24A1 promoter in both TRAP-MVNP and WT OCL precursors. We found that 1,25-(OH)<sub>2</sub>D<sub>3</sub> induced TAF12 binding to the CYP24A1 promoter in TRAP-MVNP as well as WT OCL precursors, but with both basal and induced levels of binding much higher in the TRAP-MVNP OCL precursors (Fig. 5A).

#### TAF12 interacts with ATF7

Because ATF7 interacts with TAF12, we next determined if ATF7 contributed to the effects of TAF12 on VDR responsiveness. Increased levels of ATF7 expression were detected in MVNP compared to WT lysates and were not further increased by 1,25-(OH)<sub>2</sub>D<sub>3</sub> (Fig. 6A). Expression of TAF4 was not affected by MVNP (Fig. 6A). Immunoprecipitation of lysates from OCL precursors of either WT or TRAP-MVNP with an anti-TAF12 antibody followed by blotting with an anti-ATF7 antibody or vice versa revealed that TAF12 and ATF7 physically interacted in OCL precursors

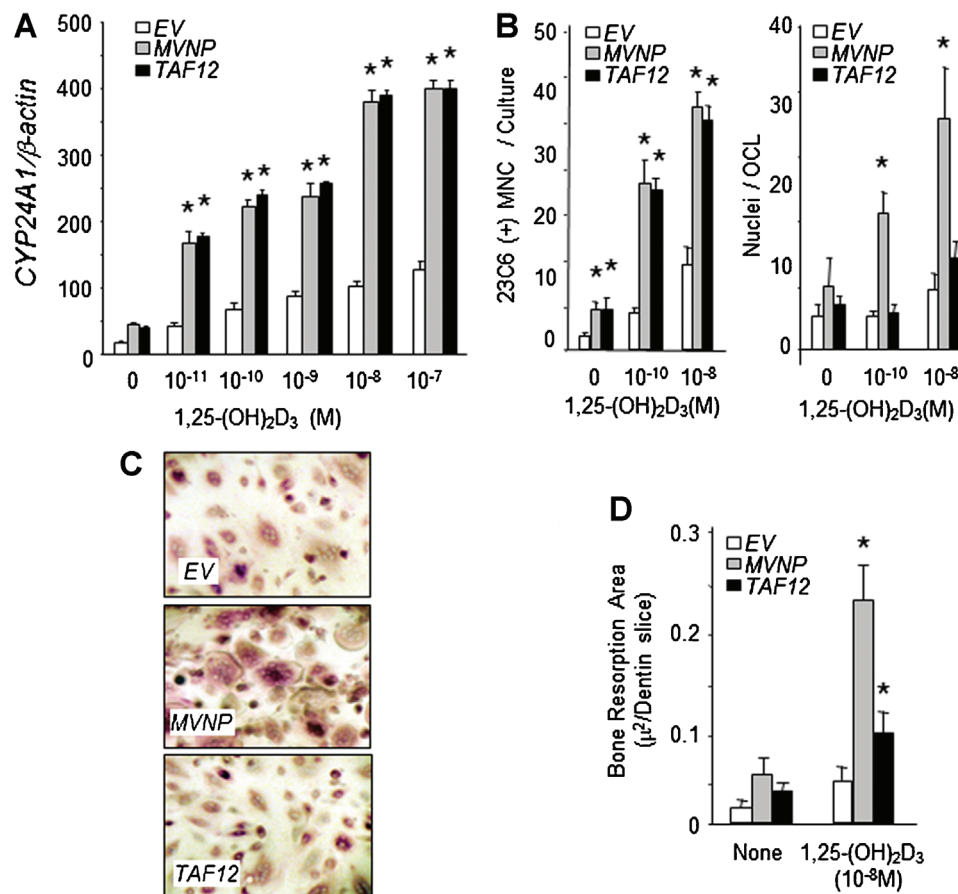


**Fig. 2.** TAF12 enhanced OCL formation, 1,25-(OH)<sub>2</sub>D<sub>3</sub> sensitivity and bone resorption by normal human OCL precursors transfected with MVNP or TAF12. (A) CYP24A1 mRNA expressions by human OCL precursors. EV, MVNP, or TAF12 transduced CFU-GM ( $5 \times 10^5$  cells) were cultured for 2 days with 1,25-(OH)<sub>2</sub>D<sub>3</sub> and then subjected to RT-PCR analysis for CYP24A1 mRNA as described. The results are expressed as mean  $\pm$  SD for triplicate cultures. \* $p < 0.01$  compared with each concentrations of 1,25-(OH)<sub>2</sub>D<sub>3</sub> treatment in EV transduced cells. (B) Number of 23C6<sup>+</sup> multinuclear cells per well. MVNP or TAF12 transduced OCL precursors ( $2 \times 10^5$ /well) treated with 1,25-(OH)<sub>2</sub>D<sub>3</sub> formed increased numbers of OCL compared to EV transduced cells. The cultures were continued for 3 weeks. The media was replaced two times per week. Multinucleated cells that cross-reacted with the 23C6 antibody and contained three or more nuclei were scored as OCLs. Data are expressed as the mean  $\pm$  SD ( $n = 4$ ). Nuclear number per OCL in marrow cultures. The number of nuclei per OCL was determined in 50 random 23C6<sup>+</sup> OCLs for each treatment group in four separate cultures, and the results are expressed as mean  $\pm$  SD. \*Significantly different from the same treatment as cells transfected with EV,  $p < 0.01$ . (C) 23C6 staining of formed osteoclasts. OCL formed from EV, MVNP, or TAF12 transduced CFU-GM. OCL precursors were treated with 1,25-(OH)<sub>2</sub>D<sub>3</sub> for 3 weeks. The media was replaced two times per week. Multinucleated cells that cross-reacted with the 23C6 antibody were scored as OCL ( $\times 200$ ). (D) Pit-forming activity of OCLs cultured on dentin slices. The cultures were overlaid with a dentin slice, and at the end of the culture period, stained with hematoxylin ( $\times 200$ ). Bone resorption areas were analyzed by the methods described.<sup>(7)</sup> Data are expressed as the mean  $\pm$  SD ( $n = 4$ ). \*Significantly different from the same treatment of cells transfected with EV,  $p < 0.01$ .

(Fig. 6B). We then examined if MVNP increased expression of phosphorylated ATF7 in OCL precursors because phosphorylated ATF7 binds TAF12. Phosphorylated ATF7 levels in MVNP mice were increased fourfold compared to WT mice at 30 minutes. (Fig. 6C). To clarify the role of ATF7 in the increased VDR responsivity induced by TAF12 and the effects TAF12 binding to VDR/VDRE, ATF7 was knocked-down in OCL precursors from TRAP-MVNP and WT with shATF7 RNA. ChIP analysis of ATF7 knockdown in OCL precursors from TRAP-MVNP mice markedly decreased TAF12 binding at the CYP24A1 promoter compared to control shRNA-transduced osteoclast precursors (Fig. 5B). Knockdown of ATF7 in OCL precursors from TRAP-MVNP mice decreased CYP24A1 sensitivity to 1,25-(OH)<sub>2</sub>D<sub>3</sub> and TAF12 levels in MVNP-expressing cells (Fig. 6D). We then examined the role of ATF7 in osteoclast formation stimulated by 1,25-(OH)<sub>2</sub>D<sub>3</sub>. Treatment of OCL precursors from MVNP or WT mice with an ATF7 shRNA significantly decreased the numbers of TRAP(+)

multinucleated cells (MNCs) (Fig. 6E). Vehicle-treated cultures did not form OCLs (data not shown).

### MVNP and TAF12 enhance VDR content

VDR content in OCL precursors from TRAP-MVNP and TRAP-TAF12 mice treated with 1,25-(OH)<sub>2</sub>D<sub>3</sub> ( $1 \times 10^{-11}$  M to  $1 \times 10^{-7}$  M) was markedly increased in both as compared to WT cells (Fig. 7A). To determine if MVNP and TAF12 increase the stability of VDR as a mechanism to enhance 1,25-(OH)<sub>2</sub>D<sub>3</sub> responsivity, we examined VDR half-life in cycloheximide-treated MVNP-transfected (MVNP-NIH3T3) and EV-transfected NIH3T3 cells (EV-NIH3T3). VDR content was quantified by Western blot. 1,25-(OH)<sub>2</sub>D<sub>3</sub> increased VDR content in both cells types, but to the same extent in MVNP-transfected and EV-transfected cells (Fig. 7B). In contrast, transfection of TAF12 small interfering RNA (siRNA), decreased VDR content (Fig. 7C).

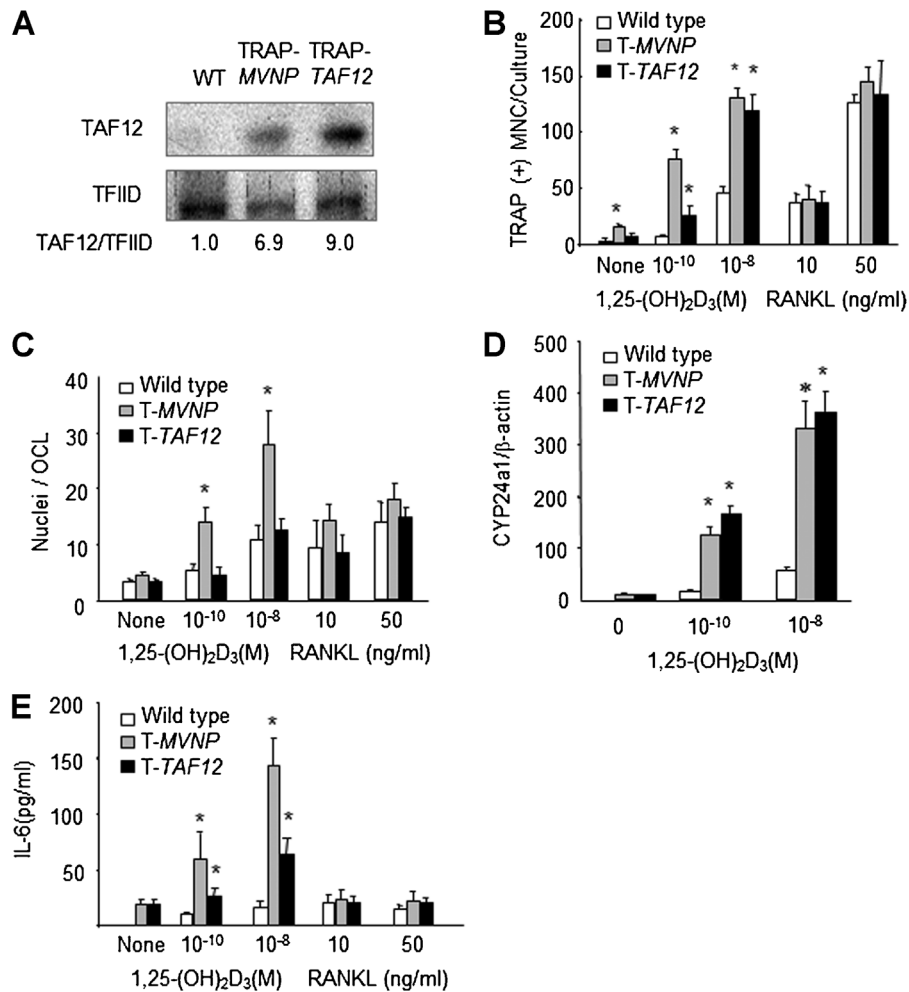


**Fig. 3.** The role of TAF12 in OCL formation by wild-type (WT), TRAP-MVNP, and TRAP-TAF12 mice. (A) TAF12 expression by OCL precursors from TRAP-TAF12 mice. CD11b<sup>+</sup> marrow mononuclear cells from WT, TRAP-MVNP, and TRAP-TAF12 mice were cultured for 2 days, then cell lysates were collected. TAF12 expression was assayed by Western blotting using an anti-TAF12 monoclonal antibody (Protein Tech Group Inc., Chicago, IL, USA). (B) OCL formation by WT, TRAP-MVNP, and TRAP-TAF12 mice. CD11b<sup>+</sup> marrow mononuclear cells from WT, TRAP-MVNP, and TRAP-TAF12 mice were cultured for 7 days with 1,25-(OH)<sub>2</sub>D<sub>3</sub> or RANKL and stained for TRAP. Cells with three or more nuclei were scored as OCLs. Results are expressed as mean ± SD (n = 4). \*Significantly different from OCL formed with the same treatment in WT mouse cultures; *p* < 0.01. (C) Nuclear number per OCL in marrow cultures. The number of nuclei per OCL was determined in 50 random TRAP<sup>+</sup> OCL for each treatment group in four separate cultures, and the results are expressed as mean ± SD. \*Significantly different from the same treatment with WT cells, *p* < 0.01. (D) CYP24A1 mRNA expressions by transgenic mouse OCL precursors. CD11b<sup>+</sup> marrow mononuclear cells from WT, TRAP-MVNP, and TRAP-TAF12 mice (5 × 10<sup>5</sup> cells) were cultured for 2 days with 1,25-(OH)<sub>2</sub>D<sub>3</sub> and then subjected to RT-PCR analysis for CYP24A1 mRNA. Total RNA from these cells was extracted using RNAzol B solution (TEL-TEST, Inc., Friendswood, TX, USA) and reverse-transcribed as follows: 5% of the first-strand cDNA pool was subjected to PCR amplification using real-time PCR promoters. The level of CYP24A1 expression by Taqman QRT-PCR analysis of total RNA isolated from TRAP-MVNP, TRAP-TAF12, or WT cells. PCR was performed for 30 cycles. The gene-specific primers for CYP24A1 mRNA were 5'-CGG GTG GAC CAT TTA CAA CTC GG-3' (sense) and 5'-CTC AAC AGG CTC ATT GTC TGT GG-3' (antisense). The gene specific designing primers for β-actin were 5'-GTG CGT GAC ATC AAA GAG-3' (sense) and 5'-GCC ACA GGA TTC CAT ACC-3' (antisense). The results are expressed as mean ± SD for triplicate cultures; \**p* < 0.01 compared with WT cells. (E) IL-6 production by OCLs from transgenic mice. CD11b<sup>+</sup> marrow mononuclear cells from WT, TRAP-MVNP, and TRAP-TAF12 mice were cultured for 7 days with 1,25-(OH)<sub>2</sub>D<sub>3</sub> or RANKL, and IL-6 production was measured in conditioned media. The production of IL-6 was assayed using specific mouse IL-6 ELISA kit (R&D). Results are expressed as mean ± SD (n = 4). \*Significantly different from OCL formed with the same treatment in WT mouse cultures; *p* < 0.01.

## Discussion

We previously reported that OCL precursors from PD patients are hypersensitive to 1,25-(OH)<sub>2</sub>D<sub>3</sub> and form OCLs at physiologic rather than pharmacologic levels of 1,25-(OH)<sub>2</sub>D<sub>3</sub>.<sup>(3)</sup> We found that the increased 1,25-(OH)<sub>2</sub>D<sub>3</sub> sensitivity was mediated by TAF12, a novel coactivator of VDR, which plays an important role in the abnormal OCL activity in PD.<sup>(7)</sup> Further, increased expression of TAF12 in NIH3T3 cells or normal marrow stromal

cells also increased their sensitivity to 1,25-(OH)<sub>2</sub>D<sub>3</sub>,<sup>(7)</sup> indicating that TAF12 can act as a VDR coactivator in multiple cell types. However, the underlying molecular mechanisms and the contribution of TAF12 to OCL activity in both normals and PD patients are unknown.

We examined the effects of blocking TAF12 expression in OCL precursors from PD patients who harbor the *p62*<sup>P392L</sup> mutation and whose OCL also express MVNP. We found that treatment with an antisense to TAF12 resulted in loss of 1,25-(OH)<sub>2</sub>D<sub>3</sub>

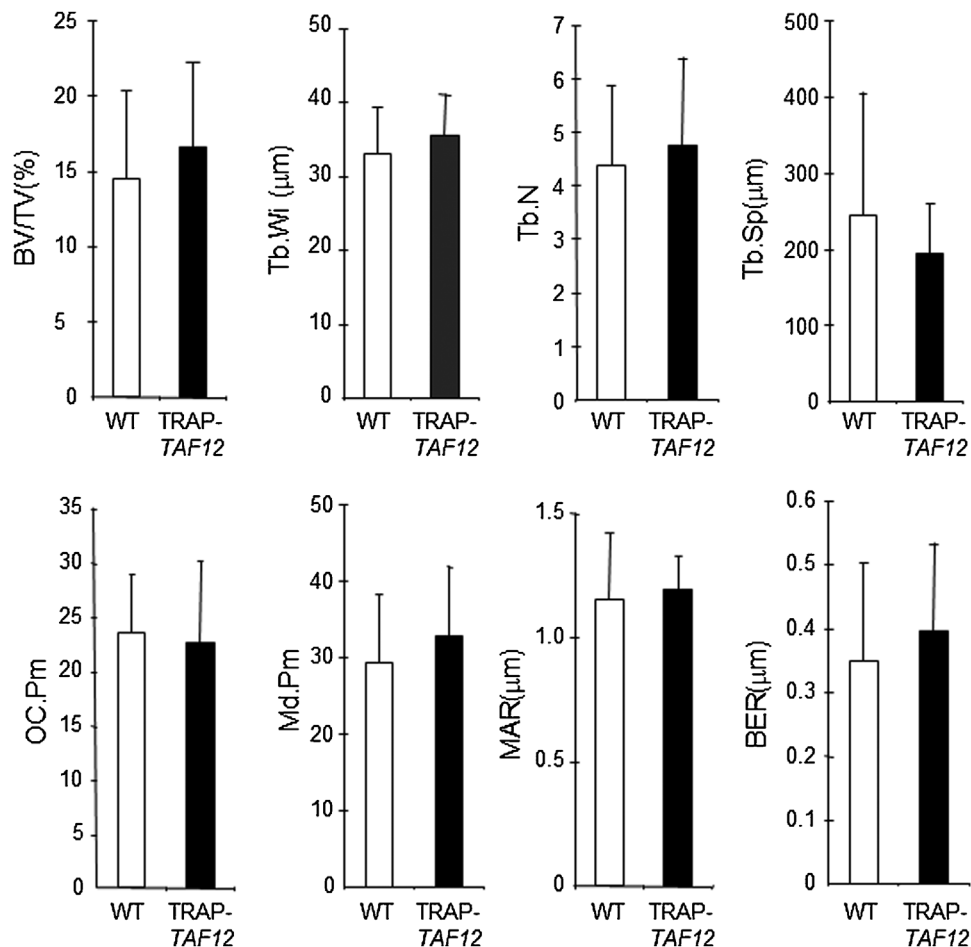


**Fig. 4.** The quantitation of  $\mu$ CT and histomorphometric analysis TRAP-TAF12 and WT mice. The fifth lumbar vertebrae ( $L_5$ ) from 12-month-old WT and TRAP-TAF12 mice were used for these analysis. Bone volume/total bone volume (BV/TV), trabecular width (Tb.Wi), trabecular number (Tb.N), trabecular bone spacing (Tb.Sp), trabecular bone thickness (2  $\mu$ m) of the OCL surface (OC.Pm), mineralized surface (Md.Pm), mineral apposition (MAR), and bone formation (BFR) rates between TRAP-TAF12 and WT mice are shown. Data represent mean  $\pm$  SD for 24 WT and 13 TRAP-TAF12 mice per group. No significant differences between WT and TRAP-TAF12 mice were detected.

hypersensitivity in OCLs from PD patients, but did not affect normal OCL function in vitro (Fig. 1). These results demonstrate that TAF12 induced by MVNP enhances the  $1,25-(OH)_2D_3$

responsivity of pagetic OCL precursors and contributes to the pagetic phenotype of OCLs from PD patients.

We then determined the effects of overexpression of TAF12 in normal OCL precursors using retroviral constructs in normal human OCL precursors. This approach allowed a direct assessment of the capacity of increased levels of TAF12 to

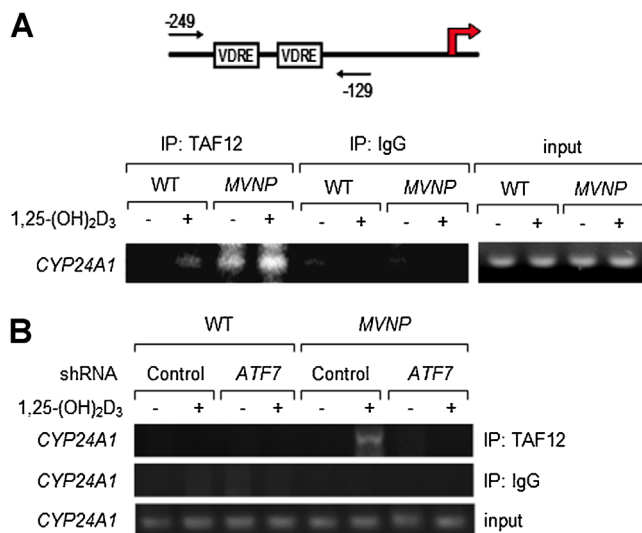
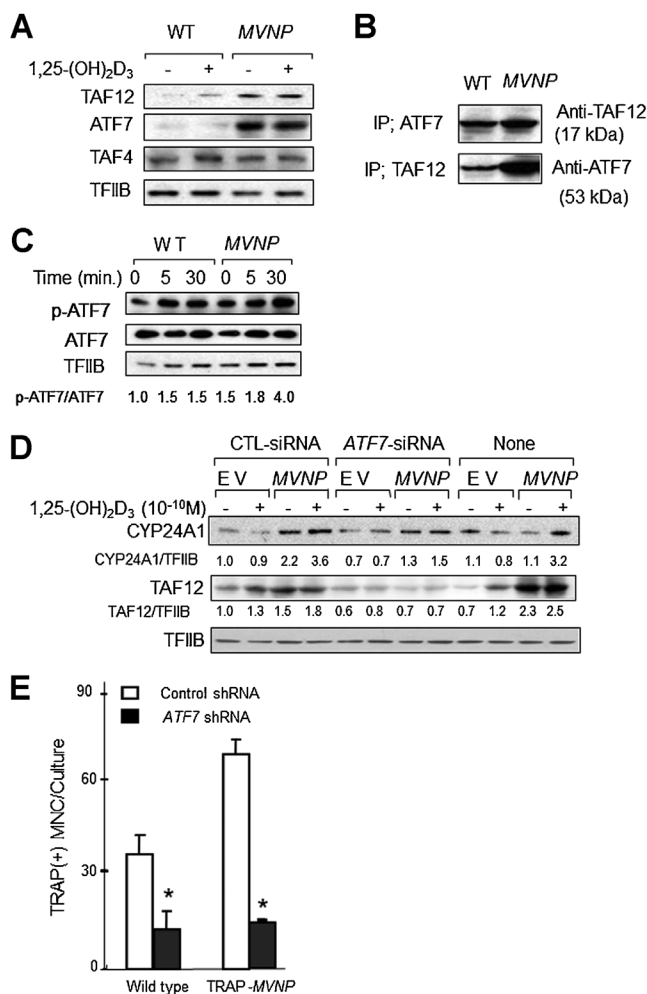


**Fig. 5.** ChIP assay demonstrating that TAF12 binds to the CYP24A1 promoter in OCL precursors from TRAP-MVNP and WT mice. (A) CD11b $^{+}$  marrow mononuclear cells from WT and TRAP-MVNP mice ( $1 \times 10^7$  cells) were cultured with  $1,25-(OH)_2D_3$  ( $1 \times 10^{-8}$  M) for 24 hours and then subjected to ChIP analysis. ChIP assays were performed using anti-TAF12 (Protein Tech Group) or anti-IgG (Santa Cruz) for control. The mouse CYP24A1 specific primers were 5'-AAG GAC ACA GAG GAA GAA GCC-3' (sense), 5'-GAA TGG CAC ACT TGG GGT AAG-3' (antisense). (B) Loss of ATF7 decreases TAF12 binding to the CYP24A1 promoter. CD11b(+) marrow mononuclear cells from WT and TRAP-MVNP mice were transduced with ATF7shRNA and cultured with  $1,25-(OH)_2D_3$  ( $1 \times 10^{-8}$  M) for 24 hours and then subjected to ChIP analysis. ChIP assays were performed using an anti-TAF12 (Protein Tech Group) or anti-IgG (Santa Cruz) for control. The mouse CYP24A1 specific primers were 5'-AAG GAC ACA GAG GAA GAA GCC-3' (sense), 5'-GAA TGG CAC ACT TGG GGT AAG-3' (antisense).

mediate  $1,25\text{-(OH)}_2\text{D}_3$  hypersensitivity of OCL precursors in vitro and to determine the potential of TAF12 to induce pagetic OCL. Both *MVNP*-transduced and *TAF12*-transduced normal human OCL precursors demonstrated increased expression of *CYP24A1* mRNA and formed increased numbers of OCL in response to  $1,25\text{-(OH)}_2\text{D}_3$  compared to *EV*-transduced OCL precursors (Fig. 2A). However, *TAF12*-transduced OCLs did not have increased numbers of nuclei per cell at low levels of  $1,25\text{-(OH)}_2\text{D}_3$  or produce the high levels of IL-6 that are characteristic of PD. High levels of IL-6 increase nuclear number per OCL and thereby the bone resorbing capacity of the OCLs. This may explain why the bone resorbing capacity of *TAF12* overexpressed OCL was not increased compared to *EV*-OCL. These results demonstrate that *TAF12* by itself cannot induce typical pagetic OCLs or induce high levels of IL-6, a characteristic of PD. Further, OCL precursors from *TRAP-TAF12* mice, which overexpress *TAF12* to a level comparable to that seen in the *TRAP-MVNP* mice, show increased responsivity of OCL precursors to  $1,25\text{-(OH)}_2\text{D}_3$  (Fig. 3B, D) and have modestly increased IL-6 production by OCL (Fig. 3E), but do not have increased nuclei/OCLs (Fig. 3C). Further, the *TRAP-TAF12* mice do not develop pagetic OCLs or bone lesions in vivo and structural variables, and osteoclast perimeter and dynamic bone formation variables were similar to those in WT mice (Fig. 4). These results demonstrate that *TAF12* increases VDR transcriptional activity, but is not sufficient to induce pagetic OCL and bone lesions characteristic of PD.



To dissect the molecular mechanisms responsible for the effects of *TAF12* on OCL formation in both WT and *TRAP-MVNP* mice, we performed ChIP analysis using an anti-*TAF12* antibody. We demonstrated that *TAF12* in the presence of  $1,25\text{-(OH)}_2\text{D}_3$  binds the *CYP24A1* promoter, which contains two functional VDREs (Fig. 5).

Next, we examined the role of *ATF7* on *TAF12*-VDR-mediated OCL activity, and the impact of loss of *ATF7* on OCL precursor responsiveness to  $1,25\text{-(OH)}_2\text{D}_3$  in vitro. *ATF7* binds as a homodimer to cyclic adenosine monophosphate (cAMP) response element (CRE) sequences (TGACGTCA) and can also heterodimerize with members of the Jun and Fos families to bind 12-O-tetradecanoylphorbol-13-acetate (TPA) response element (TRE) sequences (TGACTCAG).<sup>(24-26)</sup> Hamard and colleagues<sup>(12)</sup> reported that overexpressed *TAF12* directly interacts with *ATF7* and potentiates *ATF7*-induced transcriptional activation of *ATF7*-driven genes. Thus, *TAF12* is a functional partner of *ATF7*. We detected increased levels of *ATF7* expression in *MVNP* compared to WT OCL precursor lysates that were not further increased by  $1,25\text{-(OH)}_2\text{D}_3$ . Expression of *TAF4*<sup>(27)</sup> was not affected by *MVNP* (Fig. 6A). Coimmunoprecipitation studies revealed that *TAF12* and *ATF7* physically interact in both *TRAP-MVNP* and WT OCL

**Fig. 6.** Functional interaction between *ATF7* and *TAF12*. (A) Expression of *TAF12*, *ATF7* and *TAF4* in OCL precursors from WT and *TRAP-MVNP* mice. CD11b<sup>+</sup> marrow mononuclear cells from WT and *TRAP-MVNP* mice were cultured with  $\alpha$ -MEM-10% FCS for 3 days, and then  $1 \times 10^{-10}$  M  $1,25\text{-(OH)}_2\text{D}_3$  or vehicle was added for 48 hours. The cell lysates were collected, the nuclear fraction was isolated using a nuclear isolation kit (Active Motif) and analyzed by Western blot for effects of *MVNP* on *TAF12*, *ATF7*, and *TAF4* levels. (B) *TAF12* binds *ATF7* in OCL precursors. Cell extracts from WT and *TRAP-MVNP* OCL precursors were immunoprecipitated with an antibody against *ATF7* or *TAF12*, and the immune complexes were analyzed by Western blot with anti-*TAF12* and anti-*ATF7*, respectively. (C) Analysis of *ATF7* activation in *MVNP* and WT OCL precursors. CD11b<sup>+</sup> marrow mononuclear cells from *MVNP* and WT mice were cultured with 10 ng/mL of M-CSF in 10% FCS and  $\alpha$ -MEM for 3 days. OCL precursors from transgenic or WT mice were induced with  $1 \times 10^{-8}$  M of  $1,25\text{-(OH)}_2\text{D}_3$  for the time periods indicated, the lysates prepared and *ATF7* activation determined by Western blot analysis. The nuclear extracts (25  $\mu$ g of protein/lane) were prepared and subjected to immunoblot analysis using antibodies recognizing anti-phospho *ATF7* and anti-*ATF7* (Abcam). (D) The role of *ATF7* on transcriptional activation of *CYP24A1* and *TAF12* expression. *ATF7* knockdown experiments were performed with *MVNP* or empty vector transduced NIH3T3 cells. Control or *ATF7* siRNA was transduced into NIH3T3 cells and the cells treated with/without  $1,25\text{-(OH)}_2\text{D}_3$  for 48 hours. *CYP24A1* and *TAF12* levels were assayed by Western blot using a mouse anti-*CYP24A1* or *TAF12* monoclonal antibody. The basal ratios of *CYP24A1*/TFIIIB or *TAF12*/TFIIIB are shown as 1.0 for control siRNA transduced EV-NIH3T3 without  $1,25\text{-(OH)}_2\text{D}_3$ , and then the value of expression or suppression were calculated and compared to the basal levels. Similar results were seen in three independent experiments. The basal ratio of p-*ATF7*/ATF7 is shown as 1.0 at 0 minute; treatment of WT mice with  $1,25\text{-(OH)}_2\text{D}_3$ . (E) The role of *ATF7* in OCL formation. *ATF7* shRNA was transduced into *MVNP* and WT OCL precursors as described in Materials and Methods, the cells cultured for 7 days with  $1,25\text{-(OH)}_2\text{D}_3$ , and then the cells were stained for TRAP. TRAP<sup>+</sup> cells with three or more nuclei were scored as OCL. Results are expressed as mean  $\pm$  SD ( $n = 4$ ). \*Significantly different from OCL formed with the same treatment in WT mouse cultures;  $p < 0.01$ .

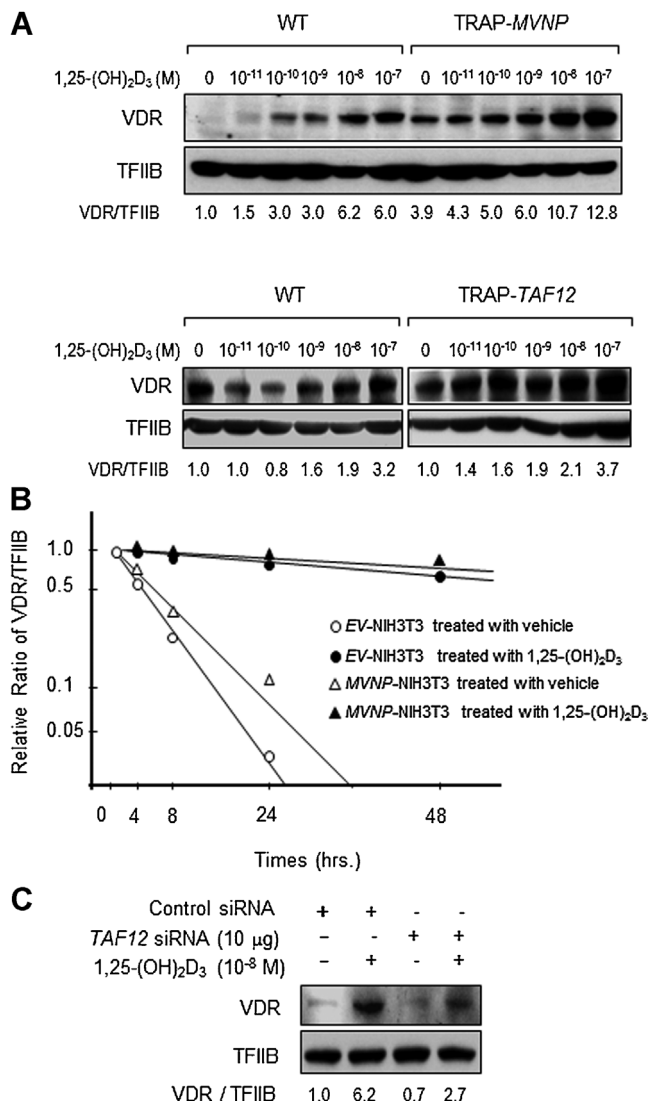


**Fig. 7.** TAF12 increases VDR content. (A) 1,25-(OH)<sub>2</sub>D<sub>3</sub> increased VDR content in OCL precursors from TRAP-MVNP and TRAP-TAF12 mice. OCL precursor cells from TRAP-MVNP, TRAP-TAF12, and WT mice were cultured for 48 hours and amounts of VDR were quantified by Western blot. The basal ratio of VDR/TFIIB is shown as 1.0 for WT cultures without 1,25-(OH)<sub>2</sub>D<sub>3</sub>, and then the ratios of VDR expression with 1,25-(OH)<sub>2</sub>D<sub>3</sub> treatment ( $1 \times 10^{-11}$  to  $1 \times 10^{-7}$  M) were calculated. (B) Effects of 1,25-(OH)<sub>2</sub>D<sub>3</sub> on VDR degradation in EV-NIH3T3 and MVNP-NIH3T3 cells treated with cyclohexamide. Time-courses for changes in VDR content in the absence or presence of 1,25-(OH)<sub>2</sub>D<sub>3</sub> ( $1 \times 10^{-10}$  M MVNP-NIH3T3;  $1 \times 10^{-8}$  M EV-NIH3T3) were examined in cells treated with cyclohexamide (10 μM). The amount of VDR was quantified by Western blot analysis using a VDR-specific monoclonal antibody. (C) Effects of TAF12 siRNA on VDR content in MVNP-transduced NIH3T3 cells. Amounts of VDR were quantified by Western blot analysis using a VDR-specific antibody after 72 hours. The basal ratio of VDR/TFIIB is shown as 1.0 for control siRNA transduced MVNP-NIH3T3 without 1,25-(OH)<sub>2</sub>D<sub>3</sub>, and then the ratios for expression or suppression were calculated.

precursors (Fig. 6B), and that the ratio of TAF12 to TAF4 is increased by MVNP, thus enhancing the ATF7-TAF12 interaction. *CYP24A1*, a key VDR target gene, is the first gene activated by VDR and deactivates 1,25-(OH)<sub>2</sub>D<sub>3</sub> to control the transcriptional activity of VDR.<sup>(28)</sup> We showed that knockdown of ATF7

decreases *CYP24A1* sensitivity to 1,25-(OH)<sub>2</sub>D<sub>3</sub> as well as TAF12 levels in MVNP-expressing cells (Fig. 6D), and knockdown of ATF7 in OCL precursors decreased OCL formation stimulated by 1,25-(OH)<sub>2</sub>D<sub>3</sub> (Fig. 6E). However, ATF7 did not bind VDR as shown by GST-VDR pull-down assays with OCL lysates (data not shown). Thus, the interaction of ATF7 with TAF12 may be involved in the upregulation of TAF12 and the resulting hypersensitivity of OCL precursors to 1,25-(OH)<sub>2</sub>D<sub>3</sub>. Recently, results presented by Hamard and colleagues<sup>(29)</sup> show that ATF7 is sumoylated in vitro and in vivo, which affects its intranuclear localization by delaying its entry into the nucleus. Sumoylation of ATF7, which affects its binding capacity to specific sequences within target promoters, was shown to be induced by binding to TAF12.<sup>(29)</sup> These reports and our results from ChIP assays (Fig. 5B) of ATF7 shRNA-treated osteoclast precursors derived from TRAP-MVNP mice show that ATF7 increases TAF12 binding to VDREs and enhances transcriptional activity on *CYP24A1*. We cannot determine from these experiments if the effects of ATF7 or TAF12 binding to *CYP24A1* simply reflect changes in the amounts of TAF12 or direct effects of ATF7 on TAF12 binding to *CYP24A1* promoter.

Results obtained using bone marrow from TRAP-MVNP and TRAP-TAF12 mice demonstrated that 1,25-(OH)<sub>2</sub>D<sub>3</sub> ( $1 \times 10^{-12}$  to  $1 \times 10^{-8}$  M) markedly increased VDR content when TAF12 expression was increased in TRAP-MVNP and TAF12 mice (Fig. 7A). 1,25-(OH)<sub>2</sub>D<sub>3</sub> also increased VDR content in both MVNP-transfected NIH3T3 cells (MVNP-NIH3T3) and EV-transfected cells (EV-NIH3T3) (Fig. 7B). Knockdown of TAF12 decreased VDR content in NIH-3T3 cells expressing MVNP (Fig. 7C). These results suggest that TAF12 also induces VDR transcription to increase VDR content, which may contribute to the 1,25-(OH)<sub>2</sub>D<sub>3</sub> hypersensitivity of OCL precursors overexpressing TAF12, although the mechanism by which it does so is unknown. Several possibilities for the roles of TAF12 and ATF7 in VDR-mediated transcription are shown in Fig. 8. Because ATF7 does

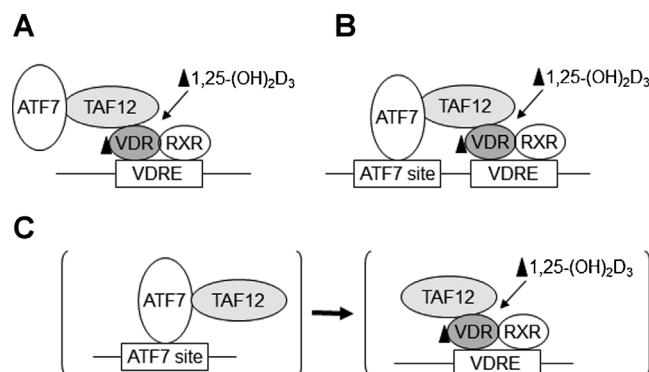


**Fig. 8.** Potential models of TAF12 recruitment to the *CYP24A1* promoter to potentiate VDR activation of transcription. It is unclear if TAF12 recruitment to the *CYP24A1* promoter is via (A, C) VDR and/or (B, C) ATF7. (A) VDR recruits TAF12, which in turn brings in ATF7 and TAF4. (B) ATF7 bound to an ATF7 site in the *CYP24A1* promoter and/or VDR bound to the VDRE recruit TAF12-TAF4. (C) ATF7 supports enhanced VDR-mediated transcription by acting at a distance from the *CYP24A1* promoter either in cis (perhaps at another *CYP24A1* regulatory region) or in trans by regulating another gene such as TAF12 that is directly involved with the VDR-mediated transcriptosome.

not bind VDR directly, it is unclear if TAF12 is recruited to the *CYP24A1* promoter by ATF7 or VDR. It is possible that VDR recruits TAF12, and the TAF12-VDR complex then brings in ATF7 to the VDRE to enhance VDR-mediated transcription (Fig. 8A). Alternatively, ATF7 could bind to an ATF7 site in the *CYP24A1* promoter that cooperates with VDR bound to the VDRE to recruit TAF12 to the promoter to enhance VDR-mediated transcription (Fig. 8B). Finally, ATF7 may support enhanced VDR-mediated transcription by binding an ATF7 site at a distance from the *CYP24A1* promoter and act either in cis (perhaps at another *CYP24A1* regulatory region) or in trans, thereby regulating another gene such as *TAF12* which is directly involved with the VDR-mediated transcriptosome.

Taken together, these results demonstrate that ATF7 and TAF12 are required for 1,25-(OH)<sub>2</sub>D<sub>3</sub> hypersensitivity of OCL precursors. Further, increased expression of TAF12 by itself is not sufficient to induce pagetic OCL precursors or pagetic bone lesions in vivo. Thus, TAF12 and other factors induced by MVNP are required for development of PD.

## Disclosures

GDR is a consultant to Amgen and develops continuing medical education material for Clinical Care Options. All other authors state that they have no conflicts of interest.

## Acknowledgments

This work was supported by NIH grant R01 AR057310 (GDR), U.S. Army Medical Research and Materials Command DOD W81XWH-12-1-0533 (NK and GDR), and research funds from the U.S. Veterans Administration (GDR).

Author's roles: GDR and NK designed the study and wrote the paper; JT, YH, SI, HI, HC, and NK performed the experiments; MAS and JJW generated the TRAP-MVNP and TRAP-TAF12 mice; JPB and LM provided PD patient bone marrow samples and expertise on Paget's disease; HZ and DWD performed histological and analysis. JJW, DWD, DLG, GDR, and NK participated in data analyses. All authors approved the final version of the manuscript.

## References

- Kanis JA. Pathophysiology and treatment of Paget's disease of bone 2nd ed. London: Martin Dunitz; 1998.
- Maldague B, Malghem J. Dynamic radiologic patterns of Paget's disease of bone. *Clin Orthop Relat Res*. 1987;217:126–51.
- Kukita A, Chenu C, McManus LM, Mundy GR, Roodman GD. Atypical multinucleated cells form in long-term marrow cultures from patients with Paget's disease. *J Clin Invest*. 1990;85:1280–6.
- Mengus G, May M, Jacq X, Staub A, Tora L, Chambon P, Davidson I. Cloning and characterization of hTAFII18, hTAFII20 and hTAFI 128: three subunits of the human transcription factor TFIID. *EMBO J*. 1995;14:1520–31.
- Mengus G, Gangloff YG, Carré L, Lavigne AC, Davidson I. The human transcription factor IID subunit human TATA-binding protein-associated factor 28 interacts in a ligand-reversible manner with the vitamin D (3) and thyroid hormone receptors. *J Biol Chem*. 2000;275:10064–71.
- Hoffmann A, Roeder RG. Cloning and characterization of human TAF20/15. Multiple interactions suggest a central role in TFIID complex formation. *J Biol Chem*. 1996;271:18194–202.
- Kurihara N, Reddy SV, Araki N, Ishizuka S, Ozono K, Cornish J, Cundy T, Singer FR, Roodman GD. Role of TAF<sub>II</sub>-17, a VDR binding protein, in the increased osteoclast formation in Paget's disease. *J Bone Miner Res*. 2004;19:1154–64.
- Kurihara N, Hiruma Y, Yamana K, Michou L, Rousseau C, Morissette J, Galson DL, Teramachi J, Zhou H, Dempster DW, Windle JJ, Brown JP, Roodman GD. Contributions of the measles virus nucleocapsid gene and the SQSTM1/p62(P392L) mutation to Paget's disease. *Cell Metab*. 2011;13:23–34.
- Kurihara N, Hiruma Y, Zhou H, Subler MA, Dempster DW, Singer FR, Reddy SV, Gruber HE, Windle JJ, Roodman GD. Mutation of the sequestosome 1 (p62) gene increases osteoclastogenesis but does not induce Paget disease. *J Clin Invest*. 2007;117:133–42.
- Kurihara N, Zhou H, Reddy SV, Garcia Palacios V, Subler MA, Dempster DW, Windle JJ, Roodman GD. Expression of measles virus nucleocapsid protein in osteoclasts induces Paget's disease-like bone lesions in mice. *J Bone Miner Res*. 2006;21:446–55.
- Hiruma Y, Kurihara N, Subler MA, Zhou H, Boykin CS, Zhang H, Ishizuka S, Dempster DW, Roodman GD, Windle JJ. A SQSTM1/p62 mutation linked to Paget's disease increases the osteoclastogenic potential of the bone microenvironment. *Hum Mol Genet*. 2008;17:3708–19.
- Hamard PJ, Dalbès-Tran R, Hauss C, Davidson I, Keding C, Chatton B. A functional interaction between ATF7 and TAF12 that is modulated by TAF4. *Oncogene*. 2005;24:3472–83.
- Voulgari A, Voskou S, Tora L, Davidson I, Sasazuki T, Shirasawa S, Pintzas A. TATA box-binding protein-associated factor 12 is important for RAS-induced transformation properties of colorectal cancer cells. *Mol Cancer Res*. 2008;6:1071–83.
- Kurihara N, Reddy SV, Menaa C, Anderson D, Roodman GD. Osteoclasts expressing the measles virus nucleocapsid gene display a pagetic phenotype. *J Clin Invest*. 2000;105:607–14.
- Reddy SV, Scarce T, Windle JJ, Leach RJ, Hundley JE, Chirgwin JM, Chou JY, Roodman GD. Cloning and characterization of the 5'-flanking region of the mouse tartrate-resistant acid phosphatase gene. *J Bone Miner Res*. 1993;8:1263–70.
- Reddy SV, Hundley JE, Windle JJ, Alcantara O, Linn R, Leach RJ, Boldt DH, Roodman GD. Characterization of the mouse tartrate-resistant acid phosphatase (TRAP) gene promoter. *J Bone Miner Res*. 1995;4:601–6.
- Nagy A, Gertsenstein M, Vintersten K, Behringer R. Manipulating the Mouse Embryo. A Laboratory Manual 3rd ed. Cold Spring Harbor, NY: CSHL Press; 2003.
- Yu S, Franceschi RT, Luo M, Fan J, Jiang D, Cao H, Kwon TG, Lai Y, Zhang J, Patrene K, Hankenson K, Roodman GD, Xiao G. Critical role of activating transcription factor 4 in the anabolic actions of parathyroid hormone in bone. *PLoS One*. 2009;4:e7583.
- Yu S, Jiang Y, Galson DL, Luo M, Lai Y, Lu Y, Ouyang HJ, Zhang J, Xiao G. General transcription factor IIA-gamma increases osteoblast-specific osteocalcin gene expression via activating transcription factor 4 and runt-related transcription factor 2. *J Biol Chem*. 2008;283:5542–3.
- Krötz F, de Wit C, Sohn HY, Zahler S, Gloe T, Pohl U, Plank C. Magnetofection—a highly efficient tool for antisense oligonucleotide delivery in vitro and in vivo. *Mol Ther*. 2003;7:700–10.
- Hofmann A, Wenzel D, Becher UM, Freitag DF, Klein AM, Eberbeck D, Schulte M, Zimmermann K, Bergemann C, Gleich B, Roell W, Weyh T, Trahms L, Nickenig G, Fleischmann BK, Pfeifer A. Combined targeting of lentiviral vectors and positioning of transduced cells by magnetic nanoparticles. *Proc Natl Acad Sci U S A*. 2009;106(1):44–9.
- Liu B, Yu SF, Li TJ. Multinucleated giant cells in various forms of giant cell containing lesions of the jaws express features of osteoclasts. *J Oral Pathol Med*. 2003;32:367–75.

23. Parfitt AM, Drezner MK, Glorieux FH, Kanis JA, Malluche H, Meunier PJ, Ott SM, Recker RR. Bone histomorphometry: standardization of nomenclature, symbols, and units. Report of the ASBMR Histomorphometry Nomenclature Committee. *J Bone Miner Res.* 1987; 2:595–610.
24. Ivashkiv LB, Liou HC, Kara CJ, Lamph WW, Verma IM, Glimcher LH. mXBP/CRE-BP2 and c-Jun form a complex which binds to the cyclic AMP, but not to the 12-O-tetradecanoylphorbol-13-acetate, response element. *Mol Cell Biol.* 1990;10:1609–21.
25. Chatton B, Bocco JL, Goetz J, Gaire M, Lutz Y, Keding C. Jun and Fos heterodimerize with ATFa, a member of the ATF/CREB family and modulate its transcriptional activity. *Oncogene.* 1994;9:375–85.
26. Chatton B, Bahr A, Acker J, Keding C. Eukaryotic GST fusion vector for the study of protein-protein associations in vivo: application to interaction of ATFa with Jun and Fos. *Biotechniques.* 1995;18:142–5.
27. Gazit K, Moshonov S, Elfakess R, Sharon M, Mengus G, Davidson I, Dikstein R. TAF4/4b  $\times$  TAF12 displays a unique mode of DNA binding and is required for core promoter function of a subset of genes. *J Biol Chem.* 2009;284:26286–96.
28. Li XY, Boudjelal M, Xiao JH, Peng ZH, Asuru A, Kang S, Fisher GJ, Voorhees JJ. 1,25-Dihydroxyvitamin D3 increases nuclear vitamin D3 receptors by blocking ubiquitin/proteasome-mediated degradation in human skin. *Mol Endocrinol.* 1999;13:1686–94.
29. Hamard PJ, Boyer-Guittaut M, Camuzeaux B, Dujardin D, Hauss C, Oelgeschläger T, Vigneron M, Keding C, Chatton B. Sumoylation delays the ATF7 transcription factor subcellular localization and inhibits its transcriptional activity. *Nucleic Acids Res.* 2007;35:1134–44.

Original Article

**Increased IL-6 Expression in Osteoclasts is Necessary but not Sufficient for  
the Development of Paget's Disease of Bone<sup>†</sup>**

Jumpei Teramachi<sup>1</sup>, Hua Zhou<sup>2</sup>, Mark A Subler<sup>3</sup>, Yukiko Kitagawa<sup>1</sup>, Deborah L Galson<sup>4</sup>, David W Dempster<sup>2</sup>, Jolene J Windle<sup>3</sup>, Noriyoshi Kurihara<sup>1</sup>, G David Roodman<sup>1, 5\*</sup>

<sup>1</sup>Department of Medicine, Hematology Oncology, Indiana University, Indianapolis, IN,

<sup>2</sup>Department of Pathology, College of Physician and Surgeons, Columbia University, New York,

NY, <sup>3</sup>Department of Human and Molecular Genetics, Virginia Commonwealth University,

Richmond, VA, <sup>4</sup>Department of Medicine, Hematology Oncology, University of Pittsburgh,

Pittsburgh, PA, <sup>5</sup>Richard L. Roudebush VA Medical Center, Indianapolis, IN

\*Corresponding author:

G. David Roodman, MD, PhD. Department of Medicine, Hematology Oncology, School of  
Medicine, Indiana University, 980 West Walnut Street , R3, Indianapolis, IN 46202 e-mail:  
groodman@iu.edu

Disclosure; GDR is a consultant to Amgen. All other authors state that they no conflicts of  
interest.

<sup>†</sup>This article has been accepted for publication and undergone full peer review but has not been through the copyediting, typesetting, pagination and proofreading process, which may lead to differences between this version and the Version of Record. Please cite this article as doi: [10.1002/jbmr.2158]

Initial Date Submitted October 2, 2013; Date Revision Submitted November 14, 2013; Date Final Disposition Set November 25, 2013

**Journal of Bone and Mineral Research**  
**© 2013 American Society for Bone and Mineral Research**  
**DOI 10.1002/jbmr.2158**

## ABSTRACT

Measles virus nucleocapsid protein (MVNP) expression in osteoclasts (OCLs) and mutation of the SQSTM1 (p62) gene contribute to the increased OCL activity in Paget's disease (PD). OCLs expressing MVNP display many of the features of PD OCLs. IL-6 production is essential for pagetic phenotype, since transgenic mice with MVNP targeted to OCLs develop pagetic OCLs and lesions, but this phenotype is absent when MVNP mice are bred to IL-6<sup>-/-</sup> mice. In contrast, mutant p62 expression in OCL precursors promotes RANKL hyper-responsivity and increased OCL production, but OCLs that form have normal morphology, are not hyper-responsive to 1,25-(OH)<sub>2</sub>D<sub>3</sub>, nor produce elevated levels of IL-6. We previously generated *p62*<sup>P394L</sup> knock-in mice (*p62KI*) and found that while OCL numbers were increased, the mice did not develop pagetic lesions. However, mice expressing both *MVNP* and *p62KI* developed more exuberant pagetic lesions than mice expressing *MVNP* alone. To examine the role of elevated IL-6 in PD and determine if MVNP mediates its effects primarily through elevation of IL-6, we generated transgenic mice that overexpress *IL-6* driven by the TRAP promoter (*TIL-6* mice) and produce IL-6 at levels comparable to *MVNP* mice. These were crossed with *p62KI* mice to determine whether *IL-6* overexpression cooperates with mutant *p62* to produce pagetic lesions. OCL precursors from *p62KI/TIL-6* mice formed greater numbers of OCLs than either *p62KI* or *TIL-6* OCL precursors in response to 1,25-(OH)<sub>2</sub>D<sub>3</sub>. Histomorphometric analysis of bones from *p62KI/TIL-6* mice revealed increased OCL numbers per bone surface area compared to WT mice. However,  $\mu$ CT analysis did not reveal significant differences between *p62KI/TIL-6* and WT mice, and no pagetic OCLs or lesions were detected in vivo. Thus, increased IL-6 expression in OCLs from *p62KI* mice contributes to increased responsivity to 1,25-(OH)<sub>2</sub>D<sub>3</sub> and increased OCL numbers, but is not sufficient to induce Paget's-like OCLs or bone lesions in vivo.

**Key Words:** p62, MVNP, IL-6, Paget's disease of bone, Osteoclasts

## Introduction

The primary cellular abnormality in Paget's disease (PD) resides in the osteoclast (OCL) <sup>(1-3)</sup>. OCLs are abundant in Paget's lesions, and are larger, contain increased nuclei/OCL, have increased bone resorbing capacity/OCL, increased 1,25-dihydroxyvitamin D<sub>3</sub> (1,25-(OH)<sub>2</sub>D<sub>3</sub>) and RANKL responsiveness, and secrete high levels of interleukin 6 (IL-6), compared to normal OCLs <sup>(4, 5)</sup>. Pagetic OCLs frequently express the measles virus nucleocapsid protein (MVNP)<sup>(6)</sup>, which we have shown induces high levels of IL-6 expression in both human and mouse OCLs, and results in the development of pagetic OCLs and pagetic bone lesions in mice in vivo <sup>(7, 8)</sup>. Further, high levels of IL-6 can induce TAF12, a VDR coactivator, in OCL precursors which increases their responsiveness to 1,25-(OH)<sub>2</sub>D<sub>3</sub>. Importantly, knockout of IL-6 in MVNP mice results in loss of their capacity to form pagetic lesions and OCLs <sup>(9)</sup>, suggests that IL-6 is required for *MVNP* to induce the development of PD.

There is also a genetic component to the etiology of PD, with up to 5-10% of all Paget's patients carrying a germline mutation in the SQSTM1/p62 gene <sup>(10)</sup>. Expression of *p62*<sup>P392L</sup>, the most frequent mutation in *p62* linked to PD in OCL precursors confers hyper-responsivity to RANKL but not 1,25-(OH)<sub>2</sub>D<sub>3</sub>, does not increase IL-6, not induce hyper-multinucleated OCLs that occur in PD. Further, we found that knock-in mice (*p62KI*) carrying a *p62*<sup>P394L</sup> mutation (the murine equivalent of the most common human PD mutation, *p62*<sup>P392L</sup>) had modestly increased OCL numbers and developed mild osteopenia, but did not develop pagetic lesions <sup>(11,12)</sup>. However, when we crossed the *p62KI* and *MVNP* mice, the resulting *p62KI/MVNP* mice developed exuberant bone lesions that closely resembled PD lesions <sup>(9)</sup>. In addition, OCL precursors isolated from *p62KI/MVNP* mice were hyper-responsive to both RANKL and 1,25-(OH)<sub>2</sub>D<sub>3</sub>, expressed elevated IL-6, and formed hyper-multinucleated OCLs that were similar to

OCL from PD patient. These results suggest that increasing IL-6 expression in OCLs of *p62KI* mice may induce pagetic lesions and a pagetic phenotype in *p62KI* mice in vivo.

To test this hypothesis, we generated transgenic mice overexpressing IL-6 in OCLs driven by the TRAP promoter (*TIL-6* mice), and crossed them with the *p62KI* mice. OCL precursors from *p62KI/TIL-6* mice were hyper-responsive to 1,25-(OH)<sub>2</sub>D<sub>3</sub> and RANKL compared to WT. However, although these OCL had increased numbers of nuclei/OCL, the nuclear number was lower than in *MVNP* mice. Further, *p62KI/TIL-6* mice did not form pagetic OCLs or bone lesions in vivo.

Paget's disease is characterized by increases in both osteoclast and osteoblast activity and we found that both of these occur in *MVNP* but not the *p62KI* mice we generated. These results raise the question of why osteoblast activity is not induced in our previously reported *p62KI* mice. We found that in contrast to *MVNP* mice, osteoblasts from *p62KI* mice expressed much lower levels of Runx2 and osterix, transcription factors necessary for osteoblast differentiation, and higher levels of DKK1, a Wnt antagonist. Treatment of osteoblast precursors from *p62KI* mice with IL-6, did not increase Runx2 or osterix and did not decrease DKK1 levels. These results suggest that *MVNP* expression in OCL induces other factors in addition to IL-6, which are necessary for the development PD lesions in mice.

## Materials and Methods

Generation of TRAP-*IL6* transgenic mice: All studies were approved by the Institutional Animal Care and Use Committees at Indiana University School of Medicine, the University of Pittsburgh School of Medicine and Virginia Commonwealth University. To generate the TRAP-*IL-6* transgene construct, a 1.1-kb EcoRI fragment containing a human *IL-6* cDNA (ATCC cDNA number 67153) was inserted into the unique EcoRI site of the pKCR3-mTRAP vector<sup>(13, 14)</sup>.

pKCR3-mTRAP contains 1.9 kb of the mouse TRAP gene promoter and 5'-UTR, in addition to rabbit  $\beta$ -globin intron 2 and its flanking exons (for efficient transgene expression). A 4.2-kb injection fragment was then excised from the TRAP-IL-6 construct with XhoI, and transgenic mice were generated by standard methods in a CB6F1 (C57Bl/6  $\times$  Balb/c) genetic background<sup>(15)</sup>. *p62KI* mice carrying a proline-to-leucine mutation at residue 394 (equivalent to human *p62*<sup>P392L</sup>) were previously described<sup>(11)</sup>. TRAP-MVNP transgenic mice were previously described<sup>(8)</sup>.

Osteoclast formation from total transgenic mouse bone marrow: Bone marrow cells flushed from long bones of WT, *p62KI*, *TIL-6*, *p62KI/TIL-6*, or *MVNP* mice were cultured in 96-well plates ( $2 \times 10^5$  cells/well) with various concentrations of 1,25-(OH) $_2$ D $_3$  (Teijin Pharma, Tokyo) or RANKL (R&D) as previously described. The end of cultures, cells were stained for TRAP using a leukocyte acid phosphatase kit (Sigma), and TRAP-positive cells ( $\geq 3$  nuclei/cell) were scored as OCLs.

Osteoclast formation from purified osteoclast precursors: OCL formation from CD11b<sup>+</sup> cells was performed as described<sup>(16)</sup>. Nonadherent cells were harvested and enriched for CD11b<sup>+</sup> mononuclear cells using the Miltenyi Biotec MACS (Magnetic Cell Sorting) system. CD11b<sup>+</sup> cells then were cultured in  $\alpha$ MEM containing 10% FCS plus 10 ng/ml of macrophage colony-stimulating factor (M-CSF; R&D Systems, Minneapolis, MN) for 3 days to generate a population of enriched early OCL precursors. These cells were then cultured in  $\alpha$ MEM containing 10% FCS in the presence of 1,25-(OH) $_2$ D $_3$  or RANKL for 3 to 4 days to generate OCLs. The cells were then stained for TRAP and TRAP-positive cells ( $\geq 3$  nuclei/cell) were scored as OCLs.

Bone resorption assays of cultured OCLs: Bone marrow cells were cultured on mammoth dentin slices (Wako, Osaka, Japan) in  $\alpha$ MEM containing 10% FCS and  $1,25\text{-(OH)}_2\text{D}_3$  ( $1 \times 10^{-8}$  M) or RANKL (100 ng/ml). After 14 days of culture, the cells were removed, the dentin slices stained with acid hematoxylin, and the areas of dentin resorption determined using image-analysis techniques (NIH ImageJ System).

Immunoblotting of OCL precursor lysates from WT, *p62KI*, *TIL-6* or *p62KI/TIL-6* mice: Total proteins were extracted from formed OCL and loaded on SDS gels (Bio-Rad Laboratories, Hercules, CA). Proteins were transferred to nitrocellulose membranes using a semi-dry blotter (Bio-Rad) and incubated in blocking solution (5% nonfat dry milk in TBST) for 1 hour. Membranes were then exposed to primary antibodies overnight at  $4^\circ\text{C}$ , and incubated with immunoglobulin G (IgG) horseradish peroxidase (HRP)-conjugated antibody for 1 hour. The blots were washed and visualized by an Immobilon Western Chemiluminescent detection system (Thermo).

RANKL ELISA assay: Mouse marrow stromal cells were isolated as previously described<sup>(11)</sup> and cultured with  $1,25\text{-(OH)}_2\text{D}_3$  for 7 days. Conditioned media from these cultures were harvested at the end of the culture period and the concentration of RANKL present was determined using an ELISA kit for mouse RANKL (R&D), according to the manufacturer's instructions.

Quantitative  $\mu$ CT measurements: The gross morphologic and microarchitectural characteristics of the distal area of the femur and  $L_5$  vertebra were examined by quantitative microcomputed

tomography ( $\mu$ CT). The L<sub>5</sub> vertebrae were used for  $\mu$ qCT to assess the trabecular bone, and the femurs were used to measure mean cortical thickness. A three-dimensional (3D) analysis was done to determine bone volume fraction (BV/TV, %), trabecular number (Tb.N, N/ $\mu$ m<sup>2</sup>), trabecular thickness (Tb.Th,  $\mu$ m), and trabecular bone spacing (Tb.Sp,  $\mu$ m). Cortical bone also was analyzed in the femur 2 mm below the growth plate, and the same segmentation parameters were used for analysis.

Bone histomorphometric analyses: Mice were given calcein (10 mg/kg) on day 7 and day 2 prior to euthanasia. Lumbar vertebrae from WT, p62KI/TIL-6 or TIL-6 mice were subjected to qualitative histological examination and histomorphometry. The decalcified sections were stained for TRAP, and OCL containing active TRAP were stained red. The undecalcified sections were left unstained for the evaluation of fluorescent labels. The analysis was performed on the cancellous bone/marrow compartment between the cranial and caudal growth plates in the vertebral bodies without lesions using the OsteoMeasure XPTM version 1.01 morphometric programs (OsteoMetrics, Inc., Atlanta, GA, USA). Osteoclasts were defined as TRAP-positive mononuclear and multinuclear cells. Osteoclast surface (Oc.S/BS), cancellous bone volume (BV/TV), trabecular thickness (Tb.Th), trabecular number (Tb.N), trabecular separation (Tb.Sp), mineralizing surface (MS/BS), mineral apposition rate (MAR), and bone formation rate (BFR/BS) were analyzed - calculated and expressed - according to the recommendations of the ASBMR Nomenclature Committee <sup>(17)</sup>.

Isolation of primary osteoblasts: After flushing out the bone marrow from tibias and femora of p62KI, MVNP and WT mice, the tibia and femurs were cultured in  $\alpha$ MEM with 10% FCS for 7-10 days. The bones were then placed in 60-mm dishes and the cultures were continued in  $\alpha$ MEM

containing 10% FCS until cells growing out of the bones formed a confluent monolayer. The original bone was removed and the out-growth cells from the bone were treated with 0.25% Trypsin and 0.05% EDTA for 10 min at 37°C. These cells were used as primary osteoblasts without further passage. The primary osteoblasts ( $2 \times 10^5$  cells/well in 6-well plates) were cultured in  $\alpha$ MEM containing 10% FCS for 3 days and then IL-6 or vehicle was added for 4 additional days. Cell lysates were collected with lysate buffer. This isolation method was previously used to establish the MC3T3-E1 cell line<sup>(18)</sup>.

von Kossa staining: Primary osteoblasts derived from WT, *p62KI* and *MVNP* mice were cultured in 10% FCS in  $\alpha$ MEM for 3 weeks with the media changed every 3 days. The cells were then fixed with 10% formaldehyde in PBS, and stained with von Kossa stain as described<sup>(19)</sup>.

Statistical analysis: For all cell culture studies, significance was evaluated using a two-tailed unpaired Student's *t* test, with  $p < 0.05$  considered to be significant.

## Results

**Characteristics of OCLs from WT, *p62KI*, *TIL-6*, *p62KI/TIL-6* and *MVNP* mice :** OCL precursors in total marrow cultures from *MVNP* mice, and to a lesser extent, *p62KI/TIL-6* mice, were hyper-responsive to  $1,25-(\text{OH})_2\text{D}_3$  compared to *p62KI*, *TIL-6* and WT mice, and formed increased numbers of OCLs at  $10^{-10}$ - $10^{-8}$  M  $1,25-(\text{OH})_2\text{D}_3$  (Fig. 1A), suggesting that *p62<sup>P394L</sup>* and *IL-6* can co-operate to promote an increased osteoclastogenic response to  $1,25-(\text{OH})_2\text{D}_3$ . OCLs from *MVNP* and *p62KI/TIL-6* mice (and *TIL-6* mice to a lesser extent) also had increased numbers of nuclei per OCL when treated with  $1,25-(\text{OH})_2\text{D}_3$ , compared to those from WT and *p62KI* mice (Fig. 1C, D). OCL precursors in marrow cultures from *MVNP*, *p62KI/TIL-6* and

*p62KI* mice also formed increased numbers of OCLs with RANKL treatment compared to *TIL-6* and WT mice (Fig. 1B), suggesting that IL-6 does not contribute significantly to RANKL responsiveness. Bone resorption in response to 1,25-(OH)<sub>2</sub>D<sub>3</sub> (10<sup>-8</sup> M) and RANKL (100 ng/ml) was comparable in marrow cultures from *MVNP* and *p62KI/TIL6* mice, which were > *p62KI* > *TIL-6* > WT (Fig. 1E).

**OCL formation by highly purified populations of OCL precursors:** OCL formation assays by highly purified populations of OCL precursors showed that only OCL precursors from *TIL-6*, *p62KI/TIL-6* and *MVNP* mice were hyper-responsive to 1,25-(OH)<sub>2</sub>D<sub>3</sub>, compared to WT and *p62KI* derived cultures (Fig. 2A), demonstrating that the increased 1,25-(OH)<sub>2</sub>D<sub>3</sub> responsiveness seen in total marrow cultures from the *p62KI* mice (Fig. 1A) resulted from effects of stromal cells in these cultures. However, the relative OCL formation in response to RANKL by pure populations of OCL precursors was identical to that from the total marrow cultures, i.e., OCL precursors from *p62KI*, *p62KI/TIL-6* and *MVNP* mice were hyper-responsive to RANKL compared to those from *TIL-6* or WT mice (Fig. 2B). The nuclear number per OCL also showed the same pattern of results as seen in OCLs formed from whole marrow cultures (Fig. 2C). These results are consistent with our previous results showing that mutant p62 contributes to RANKL hyper-responsivity directly in OCLs, while its contribution to increased 1,25-(OH)<sub>2</sub>D<sub>3</sub> responsiveness is mediated through effects on stromal cells <sup>(11)</sup>. In contrast, IL-6 contributes to 1,25-(OH)<sub>2</sub>D<sub>3</sub> responsiveness directly in OCLs, but does not appear to have an effect on OCL response to RANKL.

We recently reported that IL-6 induces expression of TAF12, a novel coactivator of VDR-mediated transcription that is increased in OCLs from PD patients and *MVNP* mice <sup>(20)</sup>. Therefore, we determined if TAF12 expression was increased in OCLs from *p62KI*, *TIL-6* and

*p62KI/TIL-6* mice. OCLs formed by highly purified OCL precursors from *TIL-6* and *p62KI/TIL-6* mice expressed elevated levels of TAF12 compared to WT (Fig. 2D). In contrast TAF12 was not increased in OCLs from *p62KI* mice.

**RANKL expression by marrow stromal cells derived from WT, *p62KI*, *TIL-6*, *p62KI/TIL-6* and *MVNP* mice:** We previously found that marrow stromal cells from *p62KI* but not *MVNP* mice have increased expression of TAF12 which resulted in enhanced RANKL production by the stromal cells when treated with low concentrations of 1,25-(OH)<sub>2</sub>D<sub>3</sub> <sup>(7, 8)</sup>. Therefore, we measured RANKL production by stromal cells from *p62KI*, *TIL-6*, *p62KI/TIL-6*, *MVNP* and WT mice. Stromal cells from *p62KI/TIL-6* and *p62KI* mice treated with 1,25-(OH)<sub>2</sub>D<sub>3</sub> produced increased levels of RANKL when treated with 10<sup>-10</sup> M 1,25-(OH)<sub>2</sub>D<sub>3</sub> (Fig. 3A). Interestingly, *p62KI/TIL-6* stromal cells produced 2-fold more secreted RANKL than *p62KI* stromal cells (Fig. 3B). Both the RANKL/OPG ratio (Fig. 3A) and TAF12 levels (Fig. 3C) were markedly increased in stromal cells from *p62KI/TIL-6* mice but not in *MVNP* mice. These results demonstrate that high levels of IL-6 produced by *TIL-6* mice also induce TAF12 in marrow stromal cells, which enhances their responsivity to 1,25-(OH)<sub>2</sub>D<sub>3</sub> and results in increased RANKL production by stromal cells from *p62KI/TIL-6* mice treated with 1,25-(OH)<sub>2</sub>D<sub>3</sub>.

Next we examined if WT, *p62KI*, *TIL-6*, *p62KI/TIL-6* and *MVNP* stromal cells differentially supported OCL formation. Stromal cells were co-cultured with CFU-GM derived cells (OCL precursors) from WT mice with 10<sup>-8</sup> M 1,25-(OH)<sub>2</sub>D<sub>3</sub> or vehicle for 7 days. As shown in Fig. 3D, stromal cells derived from *p62KI/TIL-6* mice, and to a lesser extent *p62KI* mice, had an increased capacity to support OCL formation in response to 1,25-(OH)<sub>2</sub>D<sub>3</sub>. Since stromal cells from *MVNP* mice do not express increased TAF12, they did not increase OCL formation when co-cultured with WT OCL precursors treated with 1,25-(OH)<sub>2</sub>D<sub>3</sub> (Fig. 3D).

**Bone phenotype of *p62KI/TIL-6* mice:** To determine whether coexpression of mutant *p62* and *IL-6* in the bone promote the development of pagetic lesions, we examined lumbar vertebral bone from *p62KI*, *TIL-6*, *p62KI/TIL-6* and WT mice at 12 months of age by qualitative histology and histomorphometry, and femurs and L<sub>5</sub> vertebra by  $\mu$ CT. No pagetic lesions were found in the lumbar vertebrae of any of these mice. Further,  $\mu$ qCT histomorphometric analysis revealed no significant differences between mice of any of the four genotypes in bone structural variables (cancellous BV/TV, Tb.N, Tb.Wi, Tb.Sp) (Table 1), nor in the Md.Pm, MAR, and BFR (Fig. 4). Only OCL numbers per bone surface were significantly increased in both *p62KI* and *p62KI/TIL-6* mice (Fig. 4).

**Expression of OCL fusion molecules in OCL precursors:** Since OCL precursors from *MVNP* mice and pagetic patients expressing *MVNP* form OCLs with increased nuclei per OCL, we measured the expression levels of several fusion molecules in *MVNP*, *p62KI* and WT OCL precursors treated with IL-6 for 4 days. OCLs formed from *MVNP* mice with or without IL-6 treatment had elevated expression of DC-STAMP compared with those from *p62KI* and WT mice (Fig. 5). The expression levels of ATP6v0d2 and ADAM8 were only modestly elevated in *MVNP* OCL (Fig. 5).

**Effect of IL-6 on osteoblast differentiation:** Our previous data demonstrated that IL-6 was required to increase bone formation and induce a pagetic phenotype in *MVNP* mice <sup>(4)</sup>. It was thus our hypothesis that increasing IL-6 expression in OCLs of *p62KI* mice would result in development of a pagetic bone lesions in *p62KI/TIL-6* mice. We therefore examined the effects of IL-6 on osteoblast differentiation by primary osteoblasts from *p62KI*, *MVNP* and WT mice.

We found that there was a 2-fold increase in the levels of Runx2 and Osterix in osteoblasts from *MVNP* mice compared with WT and *p62KI* mice. These parameters were not affected by IL-6 treatment of WT, *MVNP* or *p62KI* osteoblasts (Fig. 6A). In contrast, IL-6 treatment of *MVNP* osteoblasts modestly enhanced ALP expression. The levels of osteocalcin expression were not different in WT, *p62KI* and *MVNP* osteoblasts and IL-6 did not increase osteocalcin expression (Fig. 6A). Since high expression levels of Dickkopf 1 (Dkk1) can inhibit osteoblast differentiation <sup>(21)</sup>, we measured Dkk1 levels in WT, *p62KI* and *MVNP* osteoblasts. Dkk 1 expression in *p62KI* osteoblasts was elevated 2-fold and increased to 3.8-fold with IL-6 treatment (Fig. 6A). In contrast, *MVNP* and WT osteoblasts had much lower levels of Dkk1 which were not affected by IL-6 treatment (Fig.6A). OB-cadherin and ALP were decreased in the *p62KI* mice compared to WT and *MVNP*, and were inversely correlated with Dkk1 expression, which was elevated in *p62KI* compared to WT and *MVNP*, RUNX2 and Osterix were induced 2 fold in *MVNP* mice.

We then measured the mineral deposition capacity of the osteoblasts by von Kossa staining. *MVNP* osteoblast cultures showed increased numbers of calcified areas compared with cultures of *p62KI* and WT osteoblasts (Fig. 6B). These results suggest that the osteoblast differentiation capacity of osteoblast from *p62KI* mice is much lower than osteoblast from *MVNP* mice.

## Discussion

Both environmental elements and genetic causes both contribute to PD. We found that the expression of both *MVNP* and the *SQSTM1* (*p62*) mutation *P392L* in OCLs contribute to the increased OCL activity in PD, and we have reported that *p62*<sup>P392L</sup> knock-in mice do not develop pagetic lesions unless *MVNP* is also present. When *MVNP* is present with the *p62KI* mutation,

Accepted Article

mice develop exuberant pagetic lesions very similar to those seen in patients with Paget's disease of bone. However, Daroszewska and co-workers <sup>(22)</sup> reported that a similar  $p62^{P394L}$  knock-in mouse develops small focal lesions which showed increases in bone turnover with increased bone resorption and formation, disruption of the normal bone architecture and an accumulation of woven bone. The basis for the differences in these two knock-in models is unclear at this time but demonstrate that the capacity of mutant  $p62$  to induce pagetic lesions in vivo is variable. *MVNP*, but not *p62KI*, mice have increased IL-6 production and loss of IL-6 blocks the effects of *MVNP* in PD <sup>(9, 11, 12)</sup>. These results suggest *p62KI* in combination with high IL-6 in OCL may result in PD. To address this question, we generated *p62KI/TIL-6* transgenic mice by breeding *p62KI* mice to *TIL-6* mice in which over-expression of IL-6 is driven by the TRAP promoter, and characterized their OCLs and bone phenotype.

OCL precursors from *p62KI/TIL-6* mice formed OCL that expressed an intermediate pagetic phenotype in vitro (Fig. 1). The OCLs were hyper-responsive to  $1,25-(OH)_2D_3$  and RANKL, formed OCL with increased bone resorbing capacity and elevated levels of TAF12 but developed only modest multinuclearity (Figs.1-2) compared to *MVNP* mice.

In contrast, OCL precursors from *p62KI* and WT mice were not hyper-responsive to  $1,25-(OH)_2D_3$ , expressed normal levels of TAF12 and formed normal OCLs <sup>(11)</sup>. Only OCL precursors from *p62KI/TIL-6* were hyper-responsive to RANKL, whereas both *p62KI/TIL-6* and *TIL-6* cells had increased STAT3 signaling (Fig. 2D). *p62KI* and WT OCL had normal ratios of nuclei/OCL when treated with  $1,25-(OH)_2D_3$  or RANKL. These results suggested that expression of IL-6 in *p62KI* OCL precursors is required for OCLs to express a pagetic phenotype in vitro, and that high levels of IL-6 enhances OCL precursor fusion in *p62KI* mice. The enhanced OCL precursor fusion in *MVNP* mice most likely reflects the increased expression of DC-STAMP <sup>(23, 24)</sup> in their OCL precursors, which was enhanced by IL-6 treatment (Fig. 5). DC-

STAMP appears to be increased selectively in MVNP OCL precursors compared with other fusion molecules associated with increased OCL precursor fusion (e.g., D44, CD48 and ADAM8), and was not increased significantly in *p62KI* and WT OCL precursors (Fig. 5). Lee et al.<sup>(23)</sup> reported that increased NFATc1 through upregulation of c-Fos increased expression of DC-STAMP. Because IL-6 increases expression of c-Fos and NFATc1, this may explain its capacity to enhance DC-STAMP expression. ATP6v0d2 also was upregulated modestly (1.8-fold) in MVNP OCL precursors. This mostly reflects that NFATc1 can also enhance expression of this fusion molecule<sup>(24)</sup>. Further, IL-6 enhances p38 MAPK signaling in *MVNP* OCL precursors (data not shown), which may also contribute to the hyper-multinuclearity of OCLs formed in marrow cultures from *MVNP* mice. We previously reported that enhanced p38 MAPK signaling plays a critical role in the increased nuclear number per OCL in OCLs expressing the measles virus nucleocapsid gene<sup>(9)</sup>.

Marrow stromal cells from *p62KI/TIL-6* expressed higher levels of RANKL in response to 1,25-(OH)<sub>2</sub>D<sub>3</sub> than the other mouse marrow stromal cells (Fig.3A). The RANKL/OPG expression ratio in stromal cells from *p62KI/TIL-6* was increased 3.5-fold compared with WT (Fig.3A). The stromal cells from *p62KI/TIL-6* also expressed high levels of TAF12. The expression of TAF12 in stromal cells can result in hyper-responsivity to 1,25-(OH)<sub>2</sub>D<sub>3</sub> and increased VDR transcription because at high levels, TAF12 acts as a coactivator of VDR transcription<sup>(20)</sup>. Why *p62KI/TIL-6* had higher expression of RANKL compared with *p62KI* stromal cells is not clear. Possibly, *p62<sup>P394L</sup>* and IL-6 have additive effects on VDR-TAF12 mediated transcription. These findings may in part explain the enhanced RANKL production present in the marrow microenvironment of pagetic patients.

*p62KI/TIL-6* mice did not develop pagetic bone lesions or structural characteristics seen in pagetic patients. They only had increased osteoclast perimeter scores (Fig.4A). In contrast,

dynamic bone formation variables were similar to those in WT mice (Fig. 4 and Table 1). These results suggest IL-6 is not enhancing osteoblast activity. Franchimont et al report that IL-6 can modulate osteoblast proliferation, differentiation, and apoptosis and supports osteoblast generation <sup>(27)</sup>. However, as shown in Fig. 6, IL-6 only increased ALP expression in osteoblasts from *MVNP* mice. These results suggest high levels of IL-6 are not sufficient to induce the enhanced bone formation characteristic of PD.

Interestingly *p62*KI osteoblasts had increased expression of the Wnt signaling antagonist, Dkk1, which was further increased by IL-6 (Figure 6A). Naot et al previously reported increased expression of Dkk1 in osteoblast cultures from Paget's patients <sup>(28)</sup>. The canonical Wnt pathway plays a key role in regulating osteoblast proliferation and differentiation <sup>(29)</sup>. Tian et al. have suggested that the release of Dkk1 from malignant plasma cells in multiple myeloma results in an inhibition of osteoblast proliferation, accentuating the imbalance between bone formation and bone resorption and facilitating local bone loss <sup>(21)</sup>. In the *p62*KI/*TIL-6* mice, overproduction of Dkk1 in osteoblasts could have a similar effect on bone formation. Possibly increased levels of IL-6 are responsible for the overexpression of Dkk1 in PD and contribute to the development of the lytic phase of PD through further accelerating local bone turnover. These results may explain in part why *p62*KI/*TIL-6* mice did not develop pagetic lesions *in vivo*.

In summary, these results demonstrate that *p62*<sup>P394L</sup> and *IL-6* in combination increase OCL formation and activity, but are not sufficient to induce pagetic OCL and bone lesions characteristic of PD *in vivo*. Further, based on our findings that loss of IL-6 in *MVNP* mice results in loss of their pagetic phenotype, these results demonstrate that IL-6 is necessary but not sufficient to induce PD. These data further demonstrate that expression of high IL-6 in OCL confers many of characteristics of Paget's disease OCL (hyper-responsivity to 1,25-(OH)<sub>2</sub>D<sub>3</sub>, increased nuclei/OCL, increased bone resorption) but is not sufficient by itself or in combination

with  $p62^{P394L}$  to induce PD. Thus, other factors induced by *MVNP* may also be required to enhance bone formation characteristics of PD, such as coupling factors or osteoblast stimulating factors. Recently, we found that *MVNP* but not  $p62^{P394L}$  increased expression of ephrinB2/EphB4, IGF1 and semaphorin3A, suggesting *MVNP* has multiple effects beyond upregulating IL-6 to induce Paget's disease (ASBMR 2013 abstract).

### Acknowledgments

This work was supported by R01-AR057308 (GDR) and R01-AR057310 (DLG) from NIH-NIAMS, 5P30CA016059 (JJW) from NIH/NCI Cancer Center support grant and W81XWH-12-1-0533 (NK) from Department of Defense. This research project was provided the VCU transgenic/knockout Mouse Shared Resource.

Author's role: GDR and NK designed study and wrote the paper; JT, YK and NK performed the experiments; MAS and JJW generated the transgenic mice; HZ and DWD performed histological section and analysis. JJW, DWD, DLG, GDR and NK did data interpretation. All authors approved the submission of manuscript.

## Reference

1. Hosking DJ. Paget's disease of bone. *Br Med J (Clin Res Ed)*. 1981; 283:686-8.
2. Kanis JA and Simon LS. Metabolic consequences of bone turnover in Paget's disease of bone. *Clin. Orthop*. 1987; 217:26-36.
3. Siris ES, Roodman GD. Paget's Disease of Bone, Primer on the metabolic bone diseases and disorders of mineral metabolism. 2003; Chapter 82: 495-506.
4. Roodman GD, Kurihara N, Ohsaki Y et al. Interleukin 6. A potential autocrine/paracrine factor in Paget's disease of bone. *J Clin Invest*. 1992; 89:46-52.
5. Hoyland JA, Freemont AJ, Sharpe PT Interleukin-6, IL-6 receptor, and IL-6 nuclear factor gene expression in Paget's disease. *J Bone Miner Res*. 1994;1:75-80
6. Roodman GD, Windle JJ. Paget disease of bone. *J Clin Invest*. 2005; 115:200-8.
7. Kurihara N, Reddy SV, Menaa C, et al. Osteoclasts expressing the measles virus nucleocapsid gene display a pagetic phenotype. *J Clin Invest*. 2000; 105:607-14.
8. Kurihara N, Zhou H, Reddy SV, et al. Expression of measles virus nucleocapsid protein in osteoclasts induces Paget's disease-like bone lesions in mice. *J Bone Miner Res*. 2006; 21:446-55.
9. Kurihara N, Hiruma Y, Yamana K, et al. Contributions of the measles virus nucleocapsid gene and the SQSTM1/p62(P392L) mutation to Paget's disease. *Cell Metab*. 2011; 13:23-34.
10. Sundaram K, Shanmugarajan S, Rao DS, et al., Mutant p62<sup>P392L</sup> stimulation of osteoclast differentiation in Paget's disease of bone. *Endocrinology*. 2011; 152:4180-9
11. Hiruma Y, Kurihara N, Subler MA, et al.. A SQSTM1/p62 mutation linked to Paget's disease increases the osteoclastogenic potential of the bone microenvironment. *Hum Mol Genet*. 2008; 17:3708-3719.

12. Kurihara N, Hiruma Y, Zhou H, et al. Mutation of the sequestosome 1 (p62) gene increases osteoclastogenesis but does not induce Paget disease. *J Clin Invest.* 2007; 117:133-42.
13. Reddy SV, Scarcez T, Windle JJ, et al. Cloning and characterization of the 5'-flanking region of the mouse tartrate-resistant acid phosphatase gene. *J Bone Miner Res.* 1993; 8:1263-70.
14. Reddy SV, Hundley JE, Windle JJ, et al. Characterization of the mouse tartrate resistant acid phosphatase (TRAP) gene promoter. *J Bone Miner Res.* 1995; 4:601-6.
15. Nagy A, Gertsenstein M, Vintersten K, et al. *Manipulating the Mouse Embryo. A Laboratory Manual* 3rd ed. Cold Spring Harbor. NY: CSHL Press; 2003.
16. Ishizuka H, García-Palacios V, Lu G, et al. ADAM8 enhances osteoclast precursor fusion and osteoclast formation in vitro and in vivo. *J Bone Miner Res.* 2011; 26:169-181.
17. Parfitt AM, Drezner MK, Glorieux FH, et al. Bone histomorphometry: standardization of nomenclature, symbols, and units. Report of the ASBMR Histomorphometry Nomenclature Committee. *J Bone Miner Res.* 1987; 2:595-610.
18. Sudo H, Kodama HA, Amagai Y, et al. In vitro differentiation and calcification in a new clonal osteogenic cell line derived from newborn mouse calvaria. *J Cell Biol.* 1983; 96:191-8.
19. Melton, SN.; Puchtler, Holde. Chemical Mechanisms of Staining Methods: Von Kossa's Technique: What Von Kossa Really Wrote and a Modified Reaction for Selective Demonstration of Inorganic Phosphates *Journal of Histotechnology*, 1985, 1:11-3.
20. Kurihara N, Reddy SV, Araki N, et al.. Role of TAFII-17, a VDR binding protein, in the increased osteoclast formation in Paget's disease. *J Bone Miner Res.* 2004; 19:1154-64.
21. Tian E, Zhan F, Walker R, et al. The role of the Wnt-signaling antagonist DKK1 in the development of osteolytic lesions in multiple myeloma. *N Engl J Med.* 2003; 349:2483-94.

22. Daroszewska A, van 't Hof RJ, Rojas JA, et al., A point mutation in the ubiquitin-associated domain of SQSMT1 is sufficient to cause a Paget's disease-like disorder in mice. *Hum Mol Genet.* 2011; 20:2734-44.
23. Yagi M, Miyamoto T, Sawatani Y, Iwamoto K, et al. DC-STAMP is essential for cell-cell fusion in osteoclasts and foreign body giant cells. *J Exp Med.* 2005; 202:345-51.
24. Yagi M, Miyamoto T, Toyama Y, Suda T Role of DC-STAMP in cellular fusion of osteoclasts and macrophage giant cells. *J Bone Miner Metab.* 2006; 24:355-358.
25. Lee MS, Kim HS, Yeon JT, et al.. GM-CSF regulates fusion of mononuclear osteoclasts into bone-resorbing osteoclasts by activating the Ras/ERK pathway. *J Immunol.* 2009;183:3390-9.
26. Kim K, Lee SH, Ha Kim J, et al.. NFATc1 induces osteoclast fusion via up-regulation of Atp6v0d2 and the dendritic cell-specific transmembrane protein (DC-STAMP). *Mol Endocrinol.* 2008; 22:176-8.
27. Franchimont N, Wertz S, Malaise M Interleukin-6: An osteotropic factor influencing bone formation? *Bone.* 2005; 37:601-6.
28. Naot D, Bava U, Matthews B, et al.. Differential gene expression in cultured osteoblasts and bone marrow stromal cells from patients with Paget's disease of bone. *J Bone Miner Res.* 2007; 22:298-309.
29. Gong Y, Slee RB, Fukai N, et al., Osteoporosis-Pseudoglioma Syndrome Collaborative Group. LDL receptor-related protein 5 (LRP5) affects bone accrual and eye development. *Cell.* 2001; 107:513-23.

## Figure Legends

**Fig. 1.** Osteoclast formation in whole bone marrow cultures from WT, *p62KI*, *TIL-6*, *p62KI/TIL-6* and *MVNP* mice. (A) OCL formation by treatment of 1,25-(OH)<sub>2</sub>D<sub>3</sub>. Data are expressed as the mean ± S.D. (n=4). \*, p<0.01, significantly different from OCLs formed with the same treatment in WT mouse cultures. (B) OCL formation by treatment of RANKL. Data are expressed as the mean ± S.D. (n=4). \*, p<0.01, significantly different from OCLs formed with the same treatment in WT mouse cultures. (C) Phenotype of OCLs formed from mouse bone marrow cultures. OCLs formed by 1,25-(OH)<sub>2</sub>D<sub>3</sub> (10<sup>-8</sup> M) were stained for TRAP. Magnification ×100. (D) Nuclei per OCL. The nuclear numbers per OCL were randomly counted in 25 OCLs formed in 10<sup>-8</sup> M 1,25-(OH)<sub>2</sub>D<sub>3</sub> or 100 ng/ml RANKL-treated cultures as in Figs 1A and B. Data are expressed as the mean ± S.D. (n=25). \*, p<0.01, significantly different from OCLs formed with the same treatment in WT mouse cultures. (E) Bone resorption capacity of OCLs. Bone marrow cells were cultured for 7 days with 1,25-(OH)<sub>2</sub>D<sub>3</sub> (10<sup>-8</sup> M) or RANKL (100 ng/ml) on mammoth dentin slices. Values represent the amount of dentin surface resorption (%), mean ± S.D. (n=4).

**Fig. 2.** Osteoclast formation formed by CD11b<sup>+</sup> cells from WT, *p62KI*, *TIL-6*, *p62KI/TIL-6* and *MVNP* mice. (A) OCL formation by 1,25-(OH)<sub>2</sub>D<sub>3</sub>. Data are expressed as the mean ± S.D. (n=4). \*, p<0.01, significantly different from OCLs formed with the same treatment in WT mouse cultures. (B) OCL formation by RANKL. Data are expressed as the mean ± S.D. (n=4). \*, p<0.01, significantly different from OCL formed with the same treatment in WT mouse cultures. (C) Nuclei per OCL. The nuclear number per OCL was determined by randomly scoring 25 OCLs formed in 10<sup>-8</sup> M 1,25-(OH)<sub>2</sub>D<sub>3</sub> or 100 ng/ml of RANKL treated cultures. Data are expressed as the mean ± S.D. (n=25). \*, p<0.01, significantly different from OCLs formed with

the same treatment in WT mouse cultures. (D) TAF12 expression in OCLs. CD11b<sup>+</sup> mononuclear cells were treated with 10 ng/ml of M-CSF for 3 days, then cultured with RANKL (100 ng/ml) for 4 days and cell lysates were collected. TAF12 expression was analyzed by immunoblot using antibodies recognizing TAF12 (ProteinTech). TFIIB was used as a loading control

**Fig. 3.** Support of OCL formation by marrow stromal cells from WT, *p62KI*, *TIL-6*, *p62KI/TIL-6* and *MVNP* mice. (A) RANKL and OPG expression. Stromal cells from WT, *p62KI*, *TIL-6*, *p62KI/TIL-6* and *MVNP* mice were cultured with 1,25-(OH)<sub>2</sub>D<sub>3</sub> (10<sup>-8</sup> M) for 2 days, the cell lysates were collected, and the levels of RANKL and OPG were determined by Western blot analysis using anti-RANKL and anti-OPG antibodies (Santa Cruz). The ratio of RANKL/OPG expression levels from Western blots were quantitated by densitometry using WT cultures as 1.0. (B) RANKL production by mouse marrow stromal cells. Mouse marrow stromal cells were cultured with 1,25-(OH)<sub>2</sub>D<sub>3</sub> for 7 days. Conditioned media from these cultures were harvested at the end of the culture period and the concentration of RANKL present was determined. The data is shown as mean± SD (n=4). \* p<0.01 compared with WT cells cultured with the same concentration of 1,25-(OH)<sub>2</sub>D<sub>3</sub>. (C) TAF12 expression in marrow stromal cells. Stromal cells were cultured with 10%FCS in IMDM for 3 days and then cell lysates were collected. TAF12 expression was analyzed by immunoblot using a polyclonal antibody recognizing TAF12. TFIIB was used as a loading control. (D) Support of OCL formation by marrow stromal cells. Stromal cells from WT, *p62KI*, *TIL-6*, *p62KI/TIL-6* and *MVNP* mice were co-cultured with CFU-GM derived from WT mouse bone marrow in the presence of 10<sup>-8</sup> M 1,25-(OH)<sub>2</sub>D<sub>3</sub> for 7 days. The cells were then fixed and stained for TRAP, and the TRAP-positive OCLs were counted. Results are expressed as the mean ± S.D. (n=4). \*, p<0.01 compared with results in WT cultures.

**Fig. 4.** Histomorphometric analysis of WT, *TIL-6*, *p62KI* and *p62KI/TIL-6* lumbar vertebra from 12-month-old. (A) OCL surface (OC.Pm), (B) Mineralized surface (Md.Pm), (C) Mineral apposition rate (MAR), and (D) Bone formation rate (BFR) for WT, *TIL-6*, *p62KI* and *p62KI/TIL-6* mice are shown. Data represent mean  $\pm$  SD for WT (7 male, 7 females), *p62KI* (6 male, 7 females), *TIL-6* (7 male, 10 female) and *p62KI/TIL-6* (3 male, 10 female) mice per group. \*;  $p < 0.01$  significant differences between WT and *p62KI/TIL-6* mice were detected.

**Fig. 5.** The expression of fusion molecules in WT, *p62KI* and *MVNP* OCL precursors. CD11b<sup>+</sup> mononuclear cells were treated with 10 ng/ml M-CSF for 3 days, then treated with or without mouse IL-6 (10 ng/ml) (R&D) and mouse IL-6 receptor (10 ng/ml)(R&D) for 4 days. Cell lysates were analyzed by immunoblot using antibodies recognizing DC-STAMP (Cosmo Bio Co. Ltd, Tokyo), ATP6v0d2 (Abnova Co., Taipei, Taiwan), ADAM8 (Santa Cruz), and  $\beta$ -actin (Abcam) as a loading control.

**Fig. 6.** Osteoblast differentiation markers in osteoblasts derived from WT, *p62KI* and *MVNP* mice. (A) Expression of osteoblast differentiation markers. Primary osteoblasts ( $2 \times 10^5$  cells/ 35 mm dish) were cultured with or without 10 ng/ml of IL-6 for 4 days in 10% FCS in  $\alpha$ MEM. Cell lysates were analyzed by immunoblot using antibodies recognizing OB-Cadherin (Cell Signaling), alkaline phosphatase (Millipore), Runx2 (Santa Cruz), Osterix (Abcam), osteoclastin (Millipore), Dkk1 (Cell Signaling) and  $\beta$ -actin (Abcam) as loading control. (B) Calcification *in vitro*. Osteoblasts were cultured in 10% FCS with  $\alpha$ MEM for 3 weeks as described in Materials and Methods. The cells were stained with von Kossa stain ( $\times 100$ ).

## Tables

Table 1. Structural Histomorphometric Variables of WT, *p62KI*, *TIL-6* and *p62KI/TIL-6* mice.

	Male				Female			
	WT n=7	<i>TIL-6</i> n=7	<i>p62KI</i> n=6	<i>p62KI/TIL-6</i> n=3	WT n=7	<i>TIL-6</i> n=10	<i>p62KI</i> n=7	<i>p62KI/TIL-6</i> n=10
BV/TV (%)	13.4 ± 2.1	13.1 ± 5.9	13.5 ± 5.8	14.6 ± 4.5	13.3 ± 5.6	11.9 ± 4.3	10.2 ± 2.5	11.2 ± 3.9
Tb.Th (μm)	31.4 ± 3.1	33.1 ± 5.6	36.2 ± 8.5	33.1 ± 5.0	33.3 ± 4.5	35.5 ± 5.3	35.5 ± 3.6	37.1 ± 9.8
Tb.N. (1/mm <sup>2</sup> )	4.3 ± 0.4	3.8 ± 1.1	3.7 ± 1.3	4.4 ± 0.9	4.0 ± 1.6	3.5 ± 1.7	2.9 ± 0.6	3.0 ± 0.1
Tb.Sp. (μm)	204.4 ± 22.3	248.1 ± 86.0	265.4 ± 121.9	203.0 ± 48.1	239.6 ± 73.0	312.0 ± 169.1	327.1 ± 84.3	313.0 ± 84.2

Structural variables for the lumbar vertebral bodies from 12-month-old WT, *p62KI*, *TIL-6* and *p62KI/TIL-6* mice. BV/TV, Cancellous bone volume; Tb.Th, trabecular thickness; Tb.N, trabecular number; and Tb.Sp, trabecular separation. Data are expressed as mean ± SD. No significant differences between WT and other mice in all the variables.

Figure 1

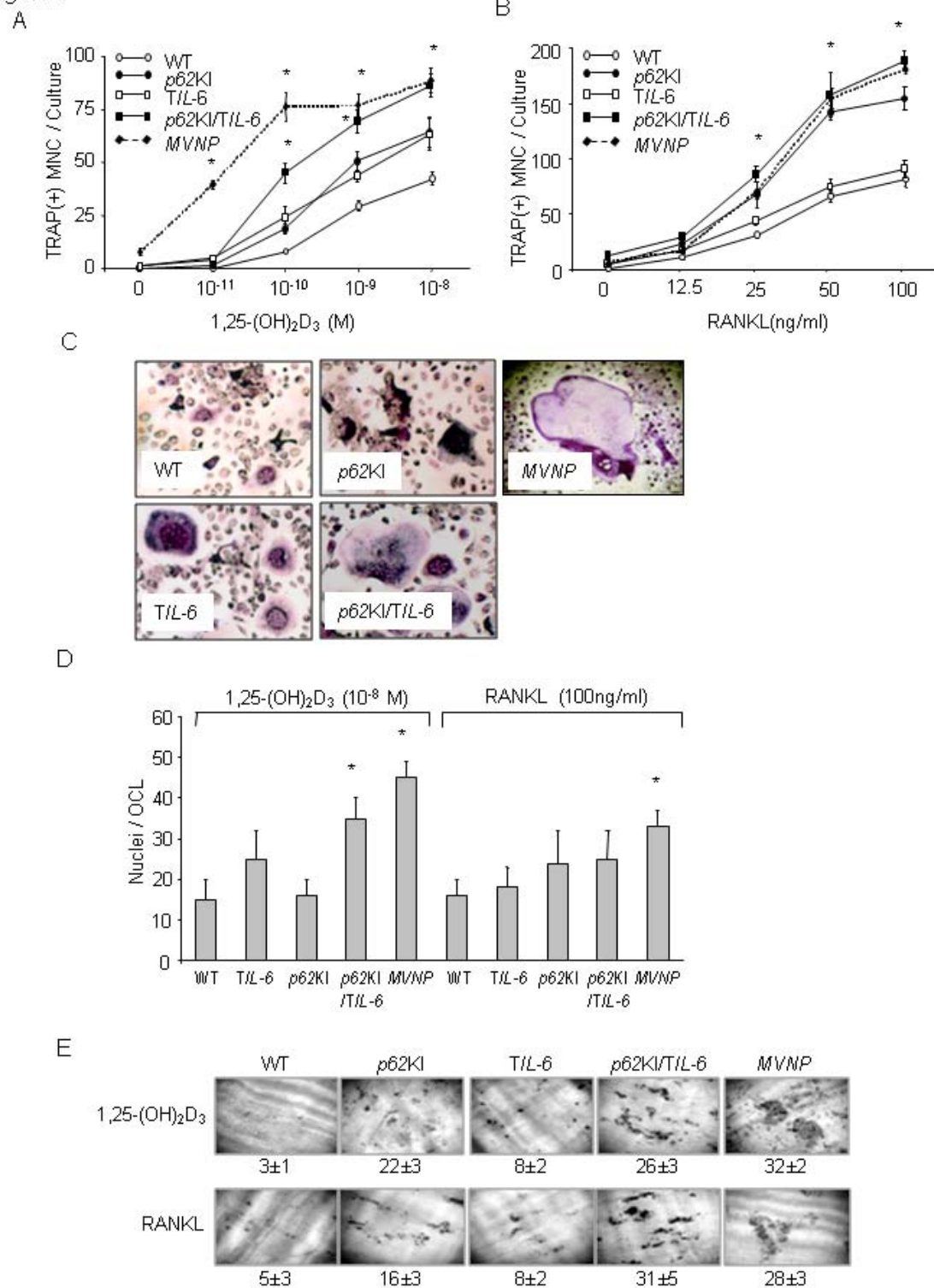


Figure 2

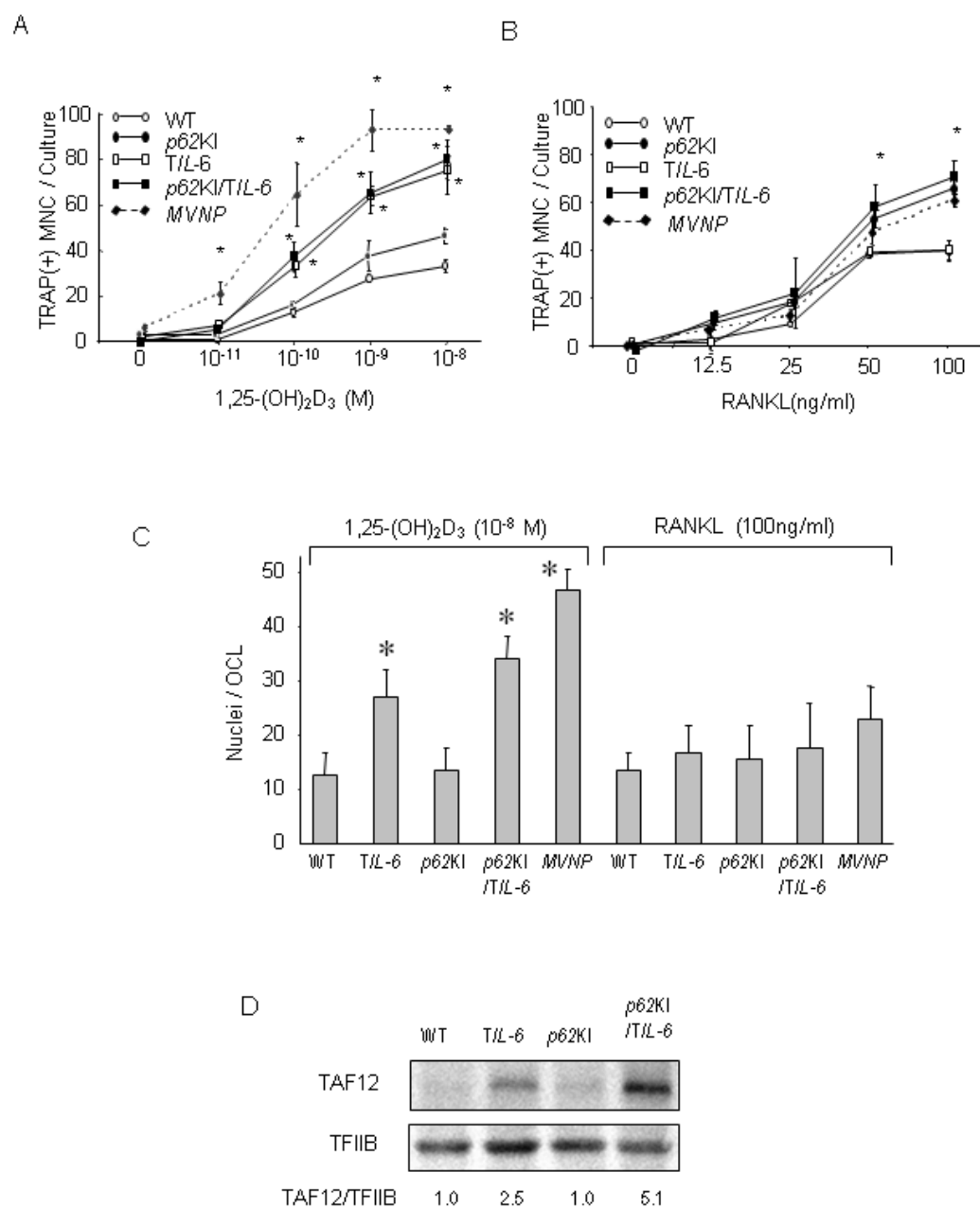


Figure 3

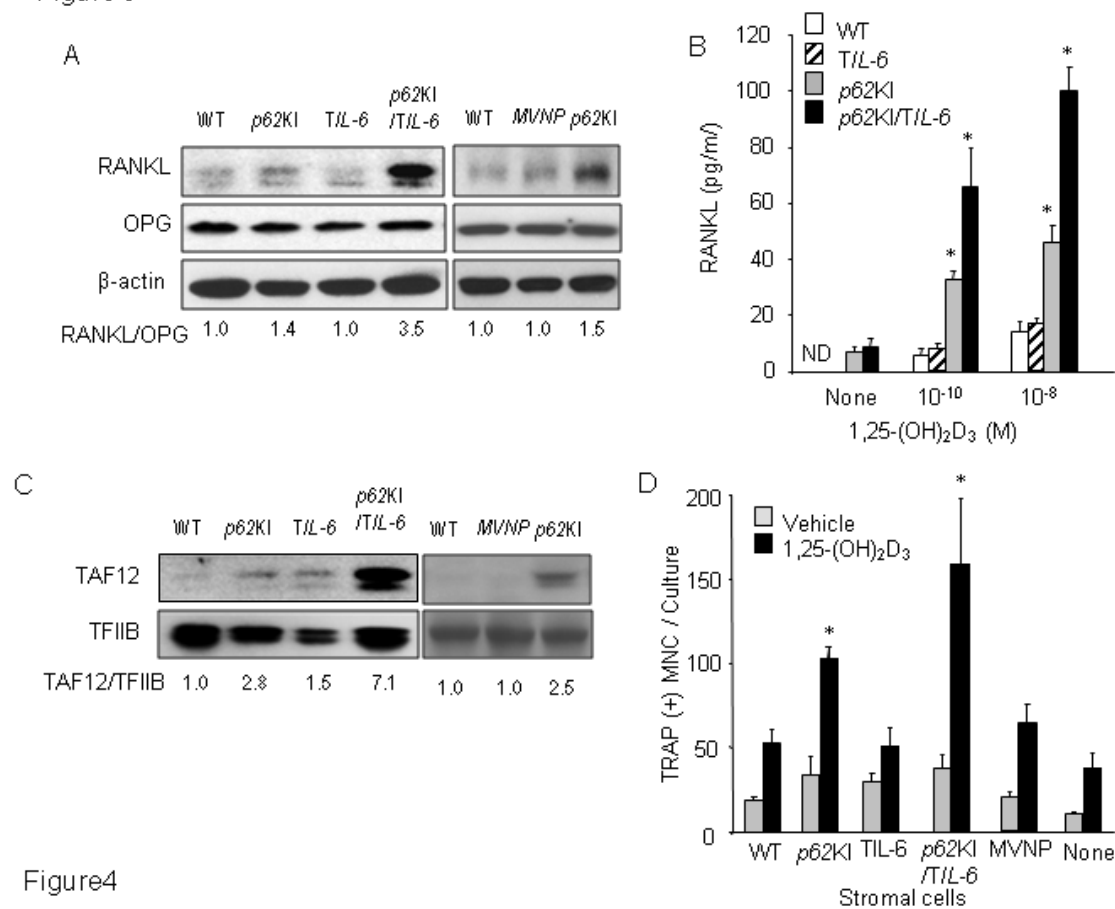


Figure 4

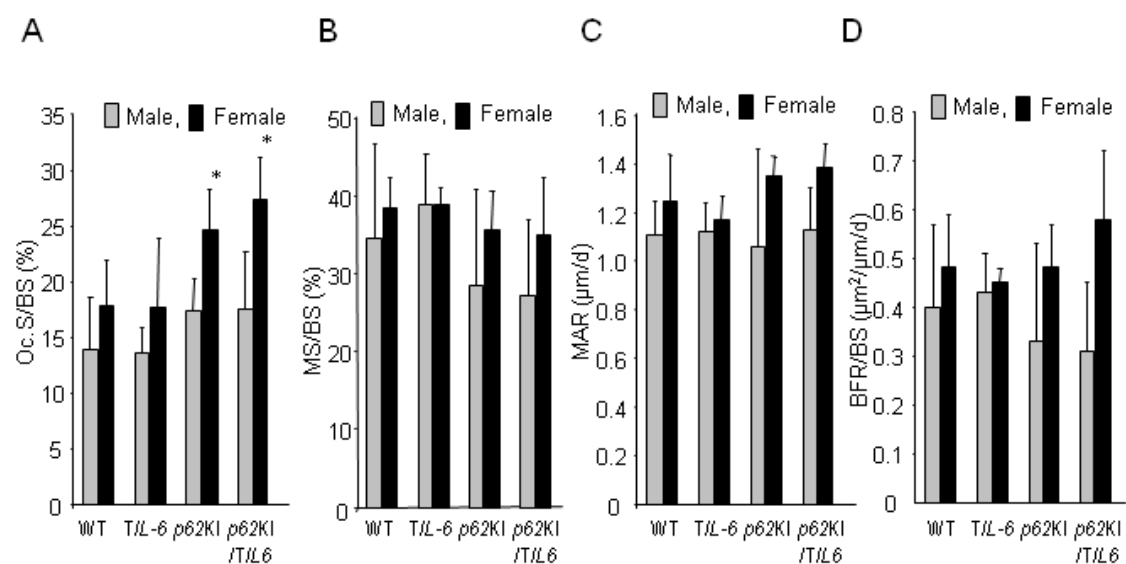


Figure 5

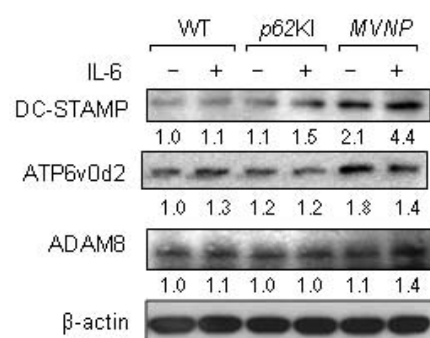
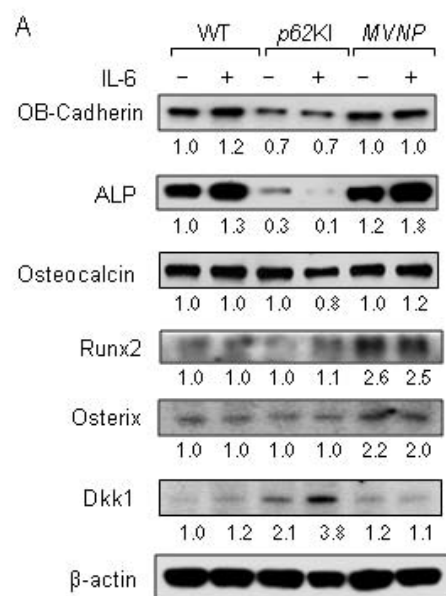


Figure 6



B

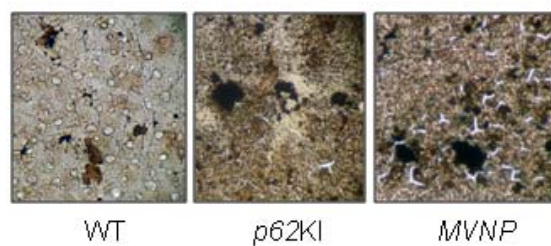


Figure 1

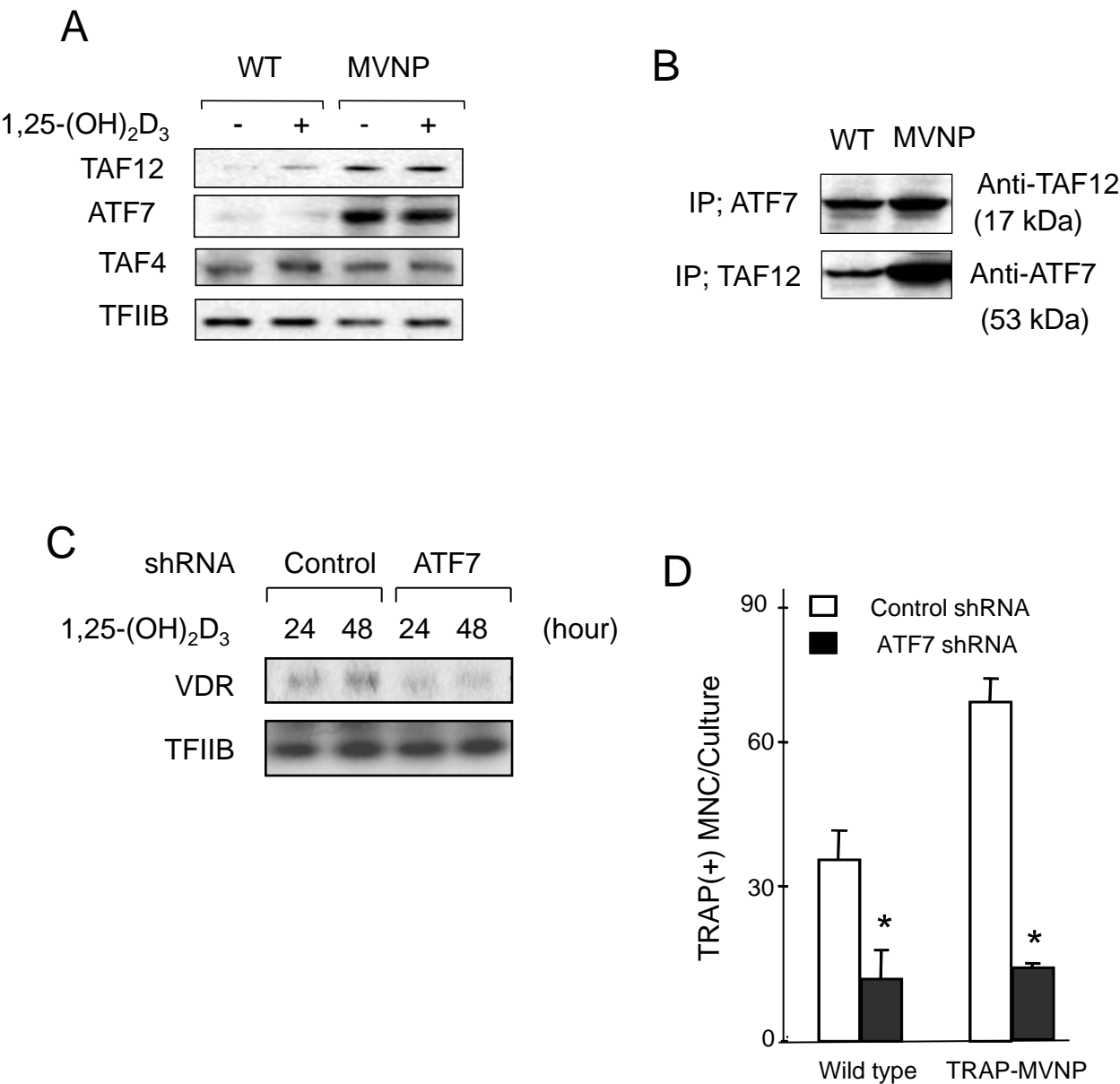


Figure 2

